

Phenomenological Study of Lepton Flavor Violation in Z Boson Decays with Constrained MSSM Extended by Type-II Seesaw Model

Vael Hajahmad^{a,b} Murhaf Alsayed Ali^c

^a*Erzincan Binali Yıldırım University,*

Faculty of Arts and Sciences, Physics Department, Erzincan, Türkiye

^b*Al-Furat University,*

Faculty of Sciences, Physics Department, Deir ez-Zor, Syria

^c*Idlib University,*

Faculty of Sciences, Physics Department, Idlib, Syria

E-mail: whahmad@erzincan.edu.tr,

morhaf.alsayed.ali@idlib-university.com

ABSTRACT: In this work, we study the lepton flavor violation (LFV) of Z boson decays in the framework of the constrained minimal supersymmetric standard model (CMSSM) extended by the type-II seesaw model. The branching ratios of $Z \rightarrow l_i l_j$ decays are calculated in this model. Here, l_i and l_j are different flavor charged leptons. After fitting to the experimental mass limits of the neutrino and supersymmetric particles, we have found that the branching ratios for LFV decays of Z boson are in the order of 6×10^{-10} for $e\mu$ channel and of 1×10^{-9} for both $\tau\mu$ and τe decay channels. Considering recent experimental constraints on $l_i \rightarrow l_j \gamma$ decays, the branching ratios for LFV decays of Z boson get an additional suppression of 10^{-8} for $e\mu$ channel and of 10^{-3} for both $\tau\mu$ and τe decay channels. The branching ratios theoretical predictions are several orders below the recent experimental limits for both scenarios, which give a very low probability to observe the LFV decays of Z boson in the future experiments.

KEYWORDS: Lepton Flavor Violation, MSSM, Type-II Seesaw Model

Contents

1	Introduction	1
2	MSSM-seesaw type-II model	3
3	The LFV decays of Z boson ($Z \rightarrow l_i l_j$)	10
4	Numerical results and discussion	13
4.1	BR($Z \rightarrow l_i l_j$) without constraints on ($l_i \rightarrow l_j \gamma$)	15
4.1.1	BR($Z \rightarrow l_i l_j$) as a function of \mathbf{A}_0 , $\tan(\beta)$, \mathbf{M}_T and $\cos(\theta_{ij})$ parameters	15
4.1.2	BR($Z \rightarrow l_i l_j$) as a contour of \mathbf{m}_0 and $\mathbf{m}_{1/2}$ parameters	17
4.2	BR($Z \rightarrow l_i l_j$) with constraints on ($l_i \rightarrow l_j \gamma$)	18
5	Conclusions	23
A	Appendix: Vertexes	24
A.1	Two Fermions - Z Boson Interactions:	24
A.2	Two Scalars - Z Boson Interactions:	25
A.3	Two Fermions - One Scalar Interactions:	25
A.4	Two Scalars - γ Interactions:	26
A.5	Two Fermions - γ Interactions:	27

1 Introduction

The Standard Model (SM) of elementary particle physics is the most successful theory for explaining many physical phenomena, which cover a wide range of energy scales that can be reached by current experiments. However, the SM cannot be considered as a complete theory due to its inability to produce masses for neutrinos [1]. Currently, one of most unsolved problems in particle physics is tiny neutrino masses, which are discovered by experiments of neutrino oscillations [2–6]. This shows that lepton flavor symmetry is not conserved in the neutrino sector [7]. The current upper limit of the neutrino mass at the Karlsruhe Tritium Neutrino Experiment (KATRIN) is estimated to be of 1.1 eV (90% CL) in 2021 [8], later on in 2022 it is estimated to be of 0.8 eV (90% CL) [9].

Theoretically, the implementation of seesaw mechanism in the standard model (SM) and supersymmetric (SUSY) looks to be the simplest solution and more motivated one to solve the problem of neutrino masses [10]. If neutrinos are Majorana particles, their mass at low energy is described by a unique dimension-5 operator [11–13]:

$$\mathcal{L}_{m_\nu} = \frac{k}{\Lambda} LLHH \quad (1.1)$$

Where Λ is the high energy scale (new physics), k a dimensionless coupling constant, L is a lepton doublet and H is a Higgs doublet [11]. By considering renormalizable interactions, there are three types of the seesaw mechanism that can be realized at the tree level. These types are called type-I, type-II and type-III which are different from each other due to the type of their seesaw messengers. In the case of type-I heavy fermionic singlets (called right-handed neutrinos) are exchanged [14–18], while in the case of type-II heavy $SU(2)_L$ scalar triplets are exchanged (the hypercharge of scalar triplet is two) [18–24]. In the type-III case, masses of neutrino are generated by exchanging of $SU(2)_L$ fermionic triplets (the hypercharge of fermionic triplets is zero) [10, 25–27].

Supersymmetry (SUSY) at the TeV scale is one of the most promising candidates for new physics beyond the standard model (BSM). It can prevent the Higgs boson mass from acquiring strong quadratic divergence corrections, realize successful gauge coupling unification and provide viable candidates to the dark matter (DM), when assuming exact R-parity by the lightest neutralino [2].

The mechanism of seesaw is a useful SUSY extension for investigation of light neutrino masses [28], which means that the energy scale of new physics is in the order of 10^{14} GeV [29]. Hence, the supersymmetric seesaw mechanism (SUSY seesaw) may induce the lepton flavor violation decays.

Lepton flavor violation (LFV) decays in the SM have a very small rate, so they are invisible in the experiments. For example, $(Z \rightarrow e \tau) \sim (Z \rightarrow e \mu) \sim 10^{-54}$ and $(Z \rightarrow \mu \tau) \sim 10^{-60}$ and $(l_j \rightarrow l_i \gamma) \leq 10^{-48}$. Thus, the charged LFV processes are forbidden in the SM [7]. This fact makes them more attractive to be considered as an important window to probe the new physics phenomena [30], thus they can be studied experimentally and theoretically using Beyond Standard Model theories (BSM). So far no LFV signal has been observed in the experiments, so upper bounds for various LFV processes are predicted [31].

The experimental upper limits of branching ratios of the three Z boson decay channels $(Z \rightarrow e \tau)$, $(Z \rightarrow \mu \tau)$ and $(Z \rightarrow e \mu)$, according to recent results of ATLAS experiment at luminosity of 139 fb^{-1} for the proton-proton collision data collected at a center of mass energy of $\sqrt{s} = 13 \text{ TeV}$ [32, 33] also for the LEP collider, are labeled in table 1.

At the future colliders e^+e^- (CEPC, FCC-ee) and at the High Luminosity Large Hadron Collider (HL-LHC), the expected sensitivity to the upper limit of branching ratios of $(Z \rightarrow e \tau)$, $(Z \rightarrow \mu \tau)$ and $(Z \rightarrow e \mu)$ are labeled in table 1. These colliders are planned to operate in the next several years at a center of mass energy near to the Z pole. Hence, it is called a Terra Z collider where the collected Z decay events will be in the order of $\sim 10^{12}$. Which is about a factor of 10^3 more than produced events at the LHC and a factor of 10^6 more than ones produced at the LEP collider [31, 34, 35].

In our study we focus on Z boson decays into two different lepton flavors ($Z \rightarrow l_i l_j$) where $l_i, l_j = e, \mu, \tau$. The work is implemented in the constrained scenario of minimal supersymmetric standard model (CMSSM) which is extended by the type-II seesaw model (adding a supersymmetric scalar triplet field).

In the SUSY seesaw model, the large flavor mixings of sleptons induce LFV interactions $l_i \bar{l}_j V$ ($V = \gamma, Z$). As a result, there will exist a correlation between branching ratios of $(Z \rightarrow l_i l_j)$ and radiative two body decays ($l_i \rightarrow l_j \gamma$) [7, 29, 36]. We consider the

Collider	LEP (95% CL)	LHC (95% CL)	HL-LHC	FCC-ee/CEPC
$BR(Z \rightarrow e\tau)$	9.8×10^{-6} [34]	7×10^{-6} [32]	10^{-6} [35]	10^{-9} [31, 34]
$BR(Z \rightarrow \mu\tau)$	1.2×10^{-5} [34]	7.20×10^{-6} [32]	10^{-6} [35]	10^{-9} [31, 34]
$BR(Z \rightarrow e\mu)$	1.7×10^{-6} [34]	2.62×10^{-7} [33]	10^{-7} [35]	$10^{-8} - 10^{-10}$ [31, 34]

Table 1. Experimental upper limits and the expected sensitivity of branching ratios of lepton flavor violating Z boson decays.

experimental bounds on both the masses of SUSY particles and the radiative two body decays ($l_i \rightarrow l_j \gamma$) to constrain the model parameters, then to evaluate the branching ratios of ($Z \rightarrow l_i l_j$) with/without imposing the constraints on ($l_i \rightarrow l_j \gamma$) decays.

2 MSSM-seesaw type-II model

In the type-II seesaw mechanism, the coupling between leptons and Higgs field is performed by exchanging of a scalar $SU(2)_L$ -triplet T [37–39]. The hypercharge of the scalar triplet T is considered to be 2 [10]. Hence, it will be set in a 15-plet for obtaining a complete representation of $SU(5)$ [10, 11, 37, 38, 40, 41]. After breaking $SU(5)$, it decomposes under $SU(3)_C \times SU(2)_L \times U(1)_Y$ to:

$$15 = \hat{S} + \hat{T} + \hat{Z}$$

$$\hat{S} \sim (6, 1, -2/3), \hat{T} \sim (1, 3, 1), \hat{Z} \sim (3, 2, 1/6)$$

Two 15-plets 15 and $\overline{15}$ are necessary for explaining the light mass of neutrino and to avoid the chiral anomalies [25, 37, 38, 42–45]. The scalar triplet T has the correct quantum numbers for generating the dimension-5 operator [11]. The breaking phase of $SU(5)$ leads to the superpotential which is below the grand unified theory scale (M_{GUT}):

$$W = W_{MSSM} + W_{SeesawII} \quad (2.1)$$

$$W_{SeesawII} = \frac{1}{\sqrt{2}} \left(Y_T \hat{L} \hat{T} \hat{L} + y_S \hat{d} \hat{S} \hat{d} \right) + Y_Z \hat{d} \hat{Z} \hat{L} + \frac{1}{\sqrt{2}} \left(\lambda_1 \hat{H}_d \hat{T} \hat{H}_d + \lambda_2 \hat{H}_u \hat{\hat{T}} \hat{H}_u \right) \\ + M_T \hat{T} \hat{\hat{T}} + M_Z \hat{Z} \hat{\hat{Z}} + M_S \hat{S} \hat{\hat{S}} \quad (2.2)$$

Where $\hat{T} = (\hat{T}^0, \hat{T}^+, \hat{T}^{++})$ and $\hat{\hat{T}} = (\hat{\hat{T}}^0, \hat{\hat{T}}^-, \hat{\hat{T}}^{--})$. The dimensionless unflavored couplings λ_1 and λ_2 are called superpotential couplings of triplets with Higgs superfields, M_T denotes the scale of heavy triplets and Y_T is the Yukawa matrix of triplets [10, 11, 42, 46, 47]. Superfields of particles in the MSSM-Seesaw type-II model are shown in table 2.

At heavy scalar triplets M_T scale, below M_{GUT} scale, the Weinberg operator is given as the following term [48]:

SF	Spin 0	Spin $\frac{1}{2}$	Generations	$(U(1) \otimes SU(2) \otimes SU(3))$
\hat{Q}	\tilde{q}	q	3	$(\frac{1}{6}, 2, 3)$
\hat{L}	\tilde{L}	L	3	$(-\frac{1}{2}, 2, 1)$
\hat{H}_d	H_d	\tilde{H}_d	1	$(-\frac{1}{2}, 2, 1)$
\hat{H}_u	H_u	\tilde{H}_u	1	$(\frac{1}{2}, 2, 1)$
\hat{d}	\tilde{d}_R^*	d_R^*	3	$(\frac{1}{3}, 1, \bar{3})$
\hat{u}	\tilde{u}_R^*	u_R^*	3	$(-\frac{2}{3}, 1, \bar{3})$
\hat{l}	\tilde{l}_R^*	l_R^*	3	$(1, 1, 1)$
\hat{T}	\tilde{T}	T	1	$(1, 3, 1)$
$\hat{\bar{T}}$	$\tilde{\bar{T}}$	\bar{T}	1	$(-1, 3, 1)$
\hat{S}	\tilde{S}	S	1	$(-\frac{2}{3}, 1, 6)$
$\hat{\bar{S}}$	$\tilde{\bar{S}}^*$	\bar{S}^*	1	$(\frac{2}{3}, 1, \bar{6})$
\hat{Z}	\tilde{Z}	Z	1	$(\frac{1}{6}, 2, 3)$
$\hat{\bar{Z}}$	$\tilde{\bar{Z}}$	\bar{Z}	1	$(-\frac{1}{6}, 2, \bar{3})$

Table 2. Chiral superfields and their quantum numbers in the MSSM-Seesaw type-II model. Here \hat{Q} , \hat{L} , \hat{H}_d and \hat{H}_u are superfields of left quarks, left leptons, down-Higgs and up-Higgs respectively. While \hat{d} , \hat{u} and \hat{l} are superfields of right down-quarks, right up-quarks and right leptons respectively.

$$\frac{1}{2}k_\nu \hat{L} \hat{L} \hat{H}_u \hat{H}_u \quad (2.3)$$

Where $k_\nu = \frac{\lambda_2}{M_T} Y_T$.

In the MSSM-Seesaw type-II model, the soft supersymmetric breaking (SUSY-breaking) terms for the heavy triplets are given as in the following equation [25, 47, 48]:

$$\begin{aligned}
-\mathcal{L}_{soft} = & \mathcal{L}_{soft-MSSM} + \frac{1}{\sqrt{2}} \left(A_T Y_T \tilde{L} \tilde{T} \tilde{L} + A_S Y_S \tilde{d}^c \tilde{S} \tilde{d}^c \right) \\
& + \frac{1}{\sqrt{2}} \left(A_1 \lambda_1 H_d \tilde{T} H_d + A_2 \lambda_2 H_u \tilde{T} H_u \right) + A_Z Y_Z \tilde{d}^c \tilde{Z} \tilde{L} \\
& + B_T M_T \tilde{T} \tilde{T} + B_Z M_Z \tilde{Z} \tilde{Z} + B_S M_S \tilde{S} \tilde{S} + h.c. \\
& + m_T^2 \tilde{T}^\dagger \tilde{T} + m_{\tilde{T}}^2 \tilde{\bar{T}}^\dagger \tilde{\bar{T}} + m_S^2 \tilde{S}^\dagger \tilde{S} + m_{\tilde{S}}^2 \tilde{\bar{S}}^\dagger \tilde{\bar{S}} + m_Z^2 \tilde{Z}^\dagger \tilde{Z} + m_{\tilde{Z}}^2 \tilde{\bar{Z}}^\dagger \tilde{\bar{Z}}
\end{aligned} \quad (2.4)$$

Where m_T^2 , m_S^2 , m_Z^2 , $m_{\tilde{T}}^2$, $m_{\tilde{S}}^2$ and $m_{\tilde{Z}}^2$ are the square of soft SUSY breaking mass terms for scalar triplets $(\tilde{T}, \tilde{\bar{T}})$, scalar singlets $(\tilde{S}, \tilde{\bar{S}})$ and scalar doublets $(\tilde{Z}, \tilde{\bar{Z}})$ respectively. A_T , A_S , A_Z , A_1 and A_2 are trilinear couplings. B_T , B_Z and B_S are bilinear couplings [25]. $\mathcal{L}_{soft, MSSM}$ for sleptons and the Gauge sector are written as:

$$\begin{aligned}
-\mathcal{L}_{soft, Slepton} = & \sum_{i,j=gen} (m_{\tilde{L}}^2)_{ij} \tilde{L}_i^* \tilde{L}_j + (m_{\tilde{l}_R}^2)_{ij} \tilde{l}_{Ri}^* \tilde{l}_{Rj} + (m_{\tilde{L}}^2)_{ij} \tilde{\nu}_{Li}^* \tilde{\nu}_{Lj} \\
& + \sum_{i,j=gen} A_{ij}^l Y_{ij}^l \tilde{l}_{Ri}^* \tilde{L}_j H_d + h.c.
\end{aligned} \tag{2.5}$$

$$-\mathcal{L}_{soft, gaugino} = \frac{1}{2} M_3 \tilde{G} \tilde{G} + \frac{1}{2} M_2 \tilde{W} \tilde{W} + \frac{1}{2} M_1 \tilde{B} \tilde{B} + h.c. \tag{2.6}$$

Where M_1 , M_2 , and M_3 represent the soft SUSY breaking mass terms for gaugino masses (bino, wino and gluino) [48, 49]. $m_{\tilde{L}}^2$ and $m_{\tilde{l}_R}^2$ represent the square of the soft SUSY breaking mass terms for supersymmetric leptons. i and j indicate to the generation number. $T_{ij}^l = A_{ij}^l Y_{ij}^l$, where A_{ij}^l are the trilinear couplings terms, h.c. is the Hermitian conjugation. The terms of squarks and Higgs are determined in the same way as in the MSSM model [49].

In the MSSM-Seesaw type-II model, after the EWSB, the mass matrices of neutralinos, sleptons and sneutrinos (taking in to account that sneutrinos are disparted into CP-odd sneutrinos and CP-even sneutrinos) are introduced as follows:

$$\tilde{\nu}_L = \frac{1}{\sqrt{2}} [\phi_L + i\sigma_L] \tag{2.7}$$

Hence, the mass matrix for CP-odd sneutrino $m_{\nu_I}^2$ is written as follows:

$$\begin{aligned}
m_{\nu_I}^2 = m_{\sigma_L \sigma_L} = & + \frac{1}{8} (g_1^2 + g_2^2) (-v_u^2 + v_d^2) + \Re(m_{\tilde{L}}^2) \\
& + \frac{1}{32} v_u^4 (2\Re(\kappa_\nu \kappa_\nu^*) + 2\Re(\kappa_\nu \kappa_\nu^\dagger) + 2\Re(\kappa_\nu^t \kappa_\nu^*) + 2\Re(\kappa_\nu^t \kappa_\nu^\dagger)) \\
& + v_d \left(-4 \left(4v_d \Re(Y_T \lambda_1^*) - v_u \mu^* (\kappa_\nu + \kappa_\nu^t + \kappa_{\nu, o_1} + \kappa_{\nu, p_1}) \right) + 8v_u \mu (\kappa_{\nu, o_1}^* + \kappa_{\nu, p_1}^*) \right)
\end{aligned} \tag{2.8}$$

Where g_1 and g_2 are gauge coupling constants of electromagnetic $U(1)_Y$ and weak $SU(2)_L$ interactions, v_u and v_d are vacuum expectation values of H_u and H_d respectively. While the indices o_1 and p_1 refer to the first generation.

The mass matrix for CP-odd sneutrino $m_{\nu_I}^2$ is diagonalized by Z^i :

$$Z^i m_{\nu_I}^2 Z^{i,\dagger} = \text{diag}(m_{\nu_1^I}^2, m_{\nu_2^I}^2, m_{\nu_3^I}^2) \tag{2.9}$$

The mass matrix for CP-even sneutrinos $m_{\nu_R}^2$ is written as:

$$\begin{aligned}
m_{\nu_R}^2 = m_{\phi_L \phi_L} = & + \frac{1}{8} (g_1^2 + g_2^2) (-v_u^2 + v_d^2) + \Re(m_{\tilde{L}}^2) \\
& + \frac{1}{32} v_u^4 (2\Re(\kappa_\nu \kappa_\nu^*) + 2\Re(\kappa_\nu \kappa_\nu^\dagger) + 2\Re(\kappa_\nu^t \kappa_\nu^*) + 2\Re(\kappa_\nu^t \kappa_\nu^\dagger)) \\
& + v_d \left(4 \left(4v_d \Re(Y_T \lambda_1^*) - v_u \mu^* (\kappa_\nu + \kappa_\nu^t + \kappa_{\nu, o_1} + \kappa_{\nu, p_1}) \right) - 8v_u \mu (\kappa_{\nu, o_1}^* + \kappa_{\nu, p_1}^*) \right)
\end{aligned} \tag{2.10}$$

The $m_{\nu_R}^2$ matrix is diagonalized by Z^R :

$$Z^R m_{\nu_R}^2 Z^{R,\dagger} = \text{diag}(m_{\tilde{\nu}_1^R}^2, m_{\tilde{\nu}_2^R}^2, m_{\tilde{\nu}_3^R}^2) \quad (2.11)$$

Where terms in the second and third lines from eqs. (2.8) and (2.10) are newly introduced by the MSSM-Seesaw type-II model. The slepton mass squared matrix is written as:

$$M_{\tilde{l}}^2 = \begin{pmatrix} M_{LL} & M_{LR} \\ M_{RL} & M_{RR} \end{pmatrix} \quad (2.12)$$

$$M_{LL} = \frac{1}{2}v_d^2 Y_l^\dagger Y_l + \frac{1}{8}(-g_2^2 + g_1^2)(-v_u^2 + v_d^2) + m_{\tilde{L}}^2 \quad (2.13)$$

$$M_{RR} = \frac{1}{2}v_d^2 Y_l Y_l^\dagger + \frac{1}{4}g_1^2(-v_d^2 + v_u^2) + m_{\tilde{l}_R}^2 \quad (2.14)$$

$$M_{LR} = \frac{1}{\sqrt{2}}(v_d T_l^\dagger - v_u \mu Y_l^\dagger) \quad (2.15)$$

$$M_{RL} = M_{LR}^\dagger = \frac{1}{\sqrt{2}}(v_d T_l - v_u Y_l \mu^*) \quad (2.16)$$

Where μ is the Higgsino mass parameter. This matrix is diagonalized by Z^E :

$$Z^E M_{\tilde{l}}^2 Z^{E,\dagger} = \text{diag}(m_{\tilde{l}_1}^2, \dots, m_{\tilde{l}_6}^2) \quad (2.17)$$

The LFV sources are off-diagonal entries of the 3×3 soft supersymmetry breaking matrices $m_{\tilde{L}}^2, m_{\tilde{l}_R}^2$. The mass matrix of neutralino can be written as:

$$m_{\tilde{\chi}^0} = \begin{pmatrix} M_1 & 0 & -\frac{1}{2}g_1 v_d & \frac{1}{2}g_1 v_u \\ 0 & M_2 & \frac{1}{2}g_2 v_d & -\frac{1}{2}g_2 v_u \\ -\frac{1}{2}g_1 v_d & \frac{1}{2}g_2 v_d & 0 & -\mu \\ \frac{1}{2}g_1 v_u & -\frac{1}{2}g_2 v_u & -\mu & 0 \end{pmatrix} \quad (2.18)$$

This matrix is diagonalized by N :

$$N^* m_{\tilde{\chi}^0} N^\dagger = \text{diag}(m_{\tilde{\chi}_1^0}, m_{\tilde{\chi}_2^0}, m_{\tilde{\chi}_3^0}, m_{\tilde{\chi}_4^0}) \quad (2.19)$$

The chargino mass matrix is given by:

$$m_{\tilde{\chi}^\pm} = \begin{pmatrix} M_2 & \frac{1}{\sqrt{2}}g_2 v_u \\ \frac{1}{\sqrt{2}}g_2 v_d & \mu \end{pmatrix} \quad (2.20)$$

This matrix is diagonalized by U and V :

$$U^* m_{\tilde{\chi}^\pm} V^\dagger = \text{diag}(m_{\tilde{\chi}_1^\pm}, m_{\tilde{\chi}_2^\pm}) \quad (2.21)$$

The flavor mixing of charged sleptons and CP-odd (CP-even) sneutrinos induces flavor-changing neutral-current couplings (FCNC) $\tilde{\chi}^0 \tilde{l} \tilde{l}$ and $Z \tilde{l} \tilde{l}$, while the flavor mixing of left-handed sneutrinos induces flavor-changing charged-current couplings $\tilde{\chi}^+ l \tilde{\nu}$. These flavor-changing couplings will contribute to the LFV of Z decays ($Z \rightarrow l_i l_j$) [29, 50] as shown in figure 1.

The mass matrix of the light neutrino is yielded by the breaking of the electroweak symmetry as in the following equation [37, 38, 51]:

$$m_\nu = \left(\frac{1}{2} v_u^2 (\kappa_\nu) \right) \quad (2.22)$$

Thus, we can write it depending on the eqs. (2.3) and (2.22) as following:

$$m_\nu = \frac{v_u^2 \lambda_2}{2 M_T} Y_T \quad (2.23)$$

This matrix is diagonalized by U^V :

$$U^{V,*} m_\nu U^{V,\dagger} = m_\nu^{dia} = \text{diag}(m_{\nu_1}, m_{\nu_2}, m_{\nu_3}) \quad (2.24)$$

The eq. (2.23) depends on the high energy scale ($M_T \sim 10^{14}$ GeV). In order to calculate the neutrino mass at low energy, we need to know values of λ_2 , M_T and Y_T as input parameters at the GUT scale $\sim 10^{16}$ GeV. Furthermore, it is obvious from the eq. (2.23) that the Y_T matrix is similar to the Y_ν matrix, because both matrices are diagonalized by the mixing matrix U^V . Thus, the structure of the Y_T matrix can be like the one of the Y_ν matrix [11, 37, 38, 48]. In principle, flavored Yukawa couplings Y_S and Y_Z are not determined by any neutrino data at low energy. However, they induce the terms of the LFV sleptons mass, as the Y_T matrix does [10].

In the general MSSM, the LFV off-diagonal entries in the slepton mass matrices involve additional free parameters which arise from the mechanism of the supersymmetry breaking. In order to relate the LFV in the slepton sector with the LFV encoded in Y_T one must assume some particular scheme for the supersymmetry breaking [11]. We will consider the constrained MSSM (CMSSM) model at the GUT scale. Hence, the supposed global conditions are as following: Soft gaugino masses combine to a common value of $M_1 = M_2 = M_3 = m_{1/2}$, the square of soft SUSY breaking masses of both supersymmetric fermions and Higgs combine to a common value of $m_{l_R}^2 = m_L^2 = m_0^2$, $m_T^2 = m_S^2 = m_Z^2 = m_{\tilde{T}}^2 = m_{\tilde{S}}^2 = m_{\tilde{Z}}^2 = m_{H_u}^2 = m_{H_d}^2 = m_0^2$ and the trilinear couplings terms combine to a common value of $A_l = A_1 = A_2 = A_0$. We have $T_{ij}^l = A_{ij}^l Y_{ij}^l$, $T_1 = A_1 \lambda_1$, $T_2 = A_2 \lambda_2$. Furthermore, m_0 is a universal scalar mass, A_0 is a universal mass parameter for the trilinear terms and $m_{1/2}$ is the common gaugino mass [11, 48].

We suppose a scenario for the trilinear terms of T, S and Z so that: $T_S = T_Z = 0$ and $T_T = A_0 Y_T$, where $Y_S = Y_Z = 0$. We suppose also for the mass terms that $M_T = M_S = M_Z$. The contribution to the mixing of supersymmetric leptons at one loop is represented by the renormalization group equations (RGEs) [48], where the lepton flavor violation occurs in the left-handed sleptons sector:

$$\begin{aligned}
\Delta m_L^2 &= -\frac{3}{8\pi^2} m_0^2 \left\{ 3 + \frac{A_0^2}{m_0^2} \right\} Y_T^\dagger Y_T \log\left(\frac{M_{GUT}}{M_T}\right) \\
\Delta T_l^2 &= \frac{-9}{16\pi^2} A_0 Y_l Y_T^\dagger Y_T \log\left(\frac{M_{GUT}}{M_T}\right) \\
\Delta m_{l_R}^2 &= 0
\end{aligned} \tag{2.25}$$

The presence of Y_T in eq. (2.25) induces LFV in the supersymmetric left-handed lepton matrix. We also notice that the terms of right-handed supersymmetric leptons do not receive any contribution to the log-decimal approximation. Furthermore, we notice that the trilinear coupling terms are suppressed by the charged lepton masses [11, 48].

We need to define the structure of the triplet Yukawa coupling matrix Y_T because of the contribution of Y_T in LFV as in eq. (2.25). We also consider real values of the Y_T matrix to avoid the possible constraints from moments of the lepton electric dipole ($Y_T^\dagger Y_T = Y_T^t Y_T$). It is effectively useful and constructive to consider a geometrical interpretation for the Yukawa coupling matrix where its elements are interpreted in the flavor space as the components of three generic (\mathbf{n}_μ , \mathbf{n}_e , \mathbf{n}_τ) neutrino vectors. We can write a Yukawa coupling matrix in flavor space as following [51, 52]:

$$Y_T = \begin{pmatrix} y_{T11} & y_{T12} & y_{T13} \\ y_{T21} & y_{T22} & y_{T23} \\ y_{T31} & y_{T32} & y_{T33} \end{pmatrix} \equiv f \begin{pmatrix} \mathbf{n}_e & \mathbf{n}_\mu & \mathbf{n}_\tau \end{pmatrix} \tag{2.26}$$

Where f is the strength of neutrino Yukawa coupling. \mathbf{n}_μ , \mathbf{n}_e and \mathbf{n}_τ are the components of three generic neutrino vectors in the flavor space. The term $Y_T^t Y_T$ in RGEs (eq. (2.25)) is related to LFV processes. We can write the term $Y_T^t Y_T$ as follows:

$$Y_T^t Y_T = f \begin{pmatrix} \mathbf{n}_e \\ \mathbf{n}_\mu \\ \mathbf{n}_\tau \end{pmatrix} f \begin{pmatrix} \mathbf{n}_e & \mathbf{n}_\mu & \mathbf{n}_\tau \end{pmatrix} = f^2 \begin{pmatrix} |n_e|^2 & \mathbf{n}_e \cdot \mathbf{n}_\mu & \mathbf{n}_e \cdot \mathbf{n}_\tau \\ \mathbf{n}_\mu \cdot \mathbf{n}_e & |n_\mu|^2 & \mathbf{n}_\mu \cdot \mathbf{n}_\tau \\ \mathbf{n}_\tau \cdot \mathbf{n}_e & \mathbf{n}_\tau \cdot \mathbf{n}_\mu & |n_\tau|^2 \end{pmatrix} \tag{2.27}$$

Where $\mathbf{n}_i \mathbf{n}_j = |n_i| |n_j| C_{ij}$. $C_{ij} \equiv \cos \theta_{ij}$ is the cosine of three neutrino flavor angles $C_{\tau\mu}$, $C_{e\mu}$ and $C_{\tau e}$. The names of the angles are induced by the certainty that the cosine of angle θ_{ij} controls the transitions of LFV in the $l_i - l_j$ sector. Therefore, the nine input parameters that determine the matrix Y_T can be considered as three modulus of the three neutrino vectors ($|n_e|, |n_\mu|, |n_\tau|$), the three relative flavor angles between these vectors are $(\theta_{\mu e}, \theta_{\tau e}, \theta_{\tau\mu})$ and the three additional angles are $(\theta_1, \theta_2, \theta_3)$ which determine the global rotation \mathcal{O} of the three neutrino vectors without changing their relative angles. Furthermore, \mathcal{O} is the orthogonal matrix of rotation and does not enter in the product $Y_T^t Y_T$ ($\mathcal{O}^t \mathcal{O} = I$) therefore it does not affect the study of LFV [51, 52]. The Y_T matrix values are real so the Yukawa matrix can be written as the product of two matrices as follows :

$$Y_T = \mathcal{O} A \tag{2.28}$$

Where the elements of the matrix A are determined according to three possible scenarios: electron-tau, tau-muon and electron-muon. For the electron-tau (ET) scenario, we substitute $C_{e\mu} = C_{\tau\mu} = 0$ in eq. (2.27) where $(\mathbf{n}_\mu, \mathbf{n}_e)$ and $(\mathbf{n}_\mu, \mathbf{n}_\tau)$ are orthogonal vectors. Thus we get:

$$Y_T^t Y_T = f^2 \begin{pmatrix} |n_e|^2 & 0 & \mathbf{n}_e \cdot \mathbf{n}_\tau \\ 0 & |n_\mu|^2 & 0 \\ \mathbf{n}_\tau \cdot \mathbf{n}_e & 0 & |n_\tau|^2 \end{pmatrix} \quad (2.29)$$

The Yukawa coupling matrix for the electron-tau scenario can be written as follows:

$$Y_{T_{e\tau}} = \mathcal{O} A_{e\tau} = \mathcal{O} f \begin{pmatrix} |n_e| & 0 & |n_\tau| C_{e\tau} \\ 0 & |n_\mu| & 0 \\ 0 & 0 & |n_\tau| \sqrt{1 - C_{e\tau}^2} \end{pmatrix} \quad (2.30)$$

By calculating the product $Y_T^t Y_T$, we get eq. (2.29). In this case, the matrix $A_{e\tau}$ is written as follows:

$$A_{e\tau} = f \begin{pmatrix} |n_e| & 0 & |n_\tau| C_{e\tau} \\ 0 & |n_\mu| & 0 \\ 0 & 0 & |n_\tau| \sqrt{1 - C_{e\tau}^2} \end{pmatrix} \quad (2.31)$$

For the tau-muon (TM) scenario, we substitute $C_{e\mu} = C_{e\tau} = 0$ in eq. (2.27) where $(\mathbf{n}_\mu, \mathbf{n}_e)$ and $(\mathbf{n}_e, \mathbf{n}_\tau)$ are orthogonal vectors. Thus the matrix of Yukawa coupling can be written as follows:

$$Y_{T_{\tau\mu}} = \mathcal{O} A_{\tau\mu} = \mathcal{O} f \begin{pmatrix} |n_e| & 0 & 0 \\ 0 & |n_\mu| & |n_\tau| C_{\tau\mu} \\ 0 & 0 & |n_\tau| \sqrt{1 - C_{\tau\mu}^2} \end{pmatrix} \quad (2.32)$$

In this case, the matrix $A_{\tau\mu}$ is written as follows:

$$A_{\tau\mu} = f \begin{pmatrix} |n_e| & 0 & 0 \\ 0 & |n_\mu| & |n_\tau| C_{\tau\mu} \\ 0 & 0 & |n_\tau| \sqrt{1 - C_{\tau\mu}^2} \end{pmatrix} \quad (2.33)$$

While for the electron-muon (EM) scenario, we substitute $C_{\tau\mu} = C_{e\tau} = 0$ in eq. (2.27) where $(\mathbf{n}_\mu, \mathbf{n}_\tau)$ and $(\mathbf{n}_\mu, \mathbf{n}_e)$ are orthogonal vectors. So, we get the matrix of Yukawa coupling in this case as follows:

$$Y_{T_{e\mu}} = \mathcal{O} A_{e\mu} = \mathcal{O} f \begin{pmatrix} |n_e| \sqrt{1 - C_{e\mu}^2} & 0 & 0 \\ |n_e| C_{e\mu} & |n_\mu| & 0 \\ 0 & 0 & |n_\tau| \end{pmatrix} \quad (2.34)$$

In this case, the matrix $A_{e\mu}$ is written as follows:

$$A_{e\mu} = f \begin{pmatrix} |n_e| \sqrt{1 - C_{e\mu}^2} & 0 & 0 \\ |n_e| C_{e\mu} & |n_\mu| & 0 \\ 0 & 0 & |n_\tau| \end{pmatrix} \quad (2.35)$$

The TM scenario ($C_{e\tau} = C_{e\mu} = 0$) may produce large rates for τ - μ transitions, but always gives negligible contributions to $\text{LFV}_{e\mu}$ and $\text{LFV}_{e\tau}$. While the ET scenario ($C_{\tau\mu} = C_{e\mu} = 0$) may give sizable rates for the τ -e transitions, but always gives negligible contributions to $\text{LFV}_{e\mu}$ and $\text{LFV}_{\tau\mu}$. The EM scenario ($C_{\tau\mu} = C_{e\tau} = 0$) may produce large rates only for the μ -e transitions [52].

3 The LFV decays of Z boson ($Z \rightarrow l_i l_j$)

The Lagrangian of the lepton flavor violation (LFV) in Z boson decays can be written as follows [45, 53]:

$$\mathcal{L}_{Zl_i l_j} = \bar{l}_j [\gamma^\mu (A_1^L P_L + A_1^R P_R) + p^\mu (A_2^L P_L + A_2^R P_R)] l_i Z_\mu$$

Where $P_{L,R} = 1/2(1 \pm \gamma^5)$ are chirality projectors, l_i and l_j represent the lepton flavors and p is the 4-momentum for l_j . The coefficients $A_1^L, A_1^R, A_2^L, A_2^R$ can be obtained from the amplitudes of Feynman diagrams as shown in figure 1. By neglecting the masses of charged leptons we can write the branching ratio equation of Z boson decays as follows [45, 53, 54]:

$$BR(Z \rightarrow l_i l_j) = BR(Z \rightarrow l_i \bar{l}_j) + BR(Z \rightarrow \bar{l}_i l_j) = \frac{\Gamma(Z \rightarrow l_i \bar{l}_j) + \Gamma(Z \rightarrow \bar{l}_i l_j)}{\Gamma_Z} \quad (3.1)$$

Γ_Z represents the total decay width of Z boson ($\Gamma_Z = 2.4952$ GeV) [55], while the decay width is given by [45, 54]:

$$\Gamma(Z \rightarrow l_i l_j) = \frac{m_Z}{48\pi} [2(|A_1^L|^2 + |A_1^R|^2) + \frac{m_Z^2}{4}(|A_2^L|^2 + |A_2^R|^2)] \quad (3.2)$$

Thus the final relation of the branching ratio can be written as follows:

$$BR(Z \rightarrow l_i l_j) = \frac{m_Z}{48\pi\Gamma_Z} [2(|A_1^L|^2 + |A_1^R|^2) + \frac{m_Z^2}{4}(|A_2^L|^2 + |A_2^R|^2)] \quad (3.3)$$

The coefficients $A_1^{L/R}$ and $A_2^{L/R}$ are combinations of the corresponding coefficients to each Feynman diagram as in figure 1. Thus, they can be expressed as:

$$\begin{aligned} A_1^{L/R} &= A_{1a}^{L/R} + A_{1b}^{L/R} + A_{1c}^{L/R} + A_{1d}^{L/R} + A_{1e}^{L/R} + A_{1f}^{L/R} + A_{1g}^{L/R} + A_{1h}^{L/R} \\ A_2^{L/R} &= A_{2a}^{L/R} + A_{2b}^{L/R} + A_{2c}^{L/R} + A_{2d}^{L/R} + A_{2e}^{L/R} + A_{2f}^{L/R} + A_{2g}^{L/R} + A_{2h}^{L/R} \end{aligned}$$

The contributions of neutralino-slepton loops are derived from figure 1(a, d, e, f), while the contributions of chargino-sneutrino loops are derived from figure 1(b, c, g, h).

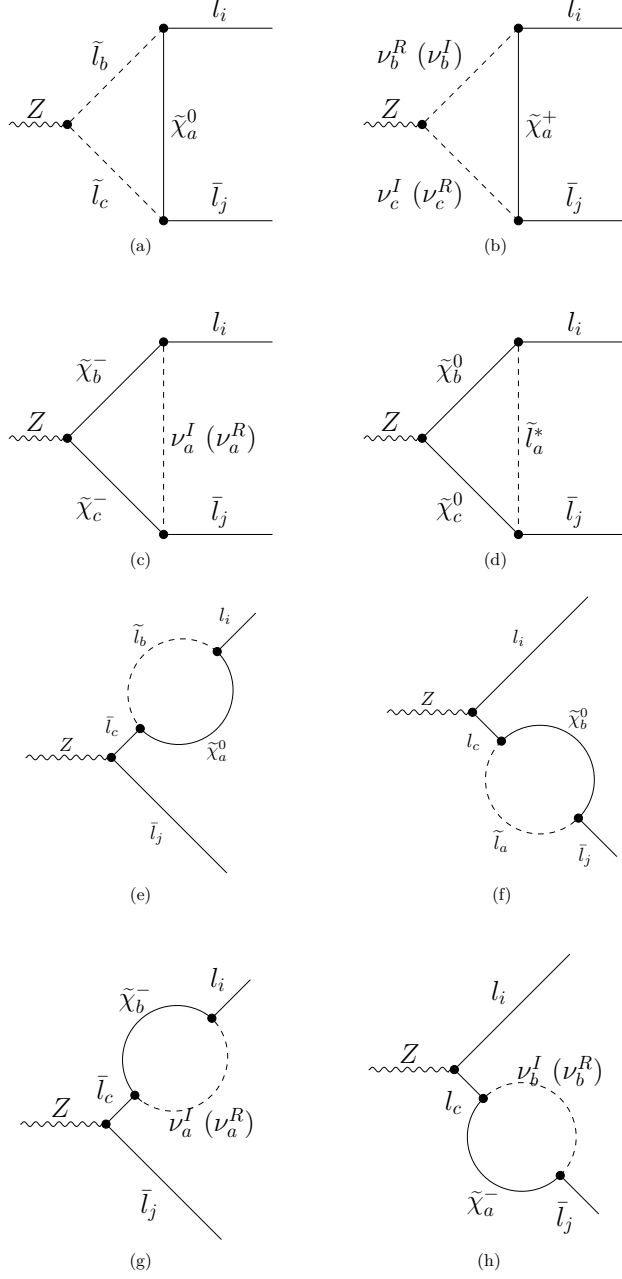


Figure 1. One loop Feynman diagrams contributing to $\text{BR}(Z \rightarrow l_i \bar{l}_j)$ in the MSSM-Seesaw type-II model. These diagrams take more important role than the others.

The contributions of figure 1(a, b) are:

$$A_1^{L(a,b)} = -2V_1^L V_2^R (-V_Z)C_{00} \quad (3.4)$$

$$A_2^{L(a,b)} = -2V_1^L V_2^L (-V_Z)(C_0 + C_1 + C_2)M \quad (3.5)$$

$$A_1^R = A_1^L(L \leftrightarrow R), A_2^R = A_2^L(L \leftrightarrow R) \quad (3.6)$$

The couplings corresponding to figure 1(a) are: $V_1^L = \Gamma_{a,i,b}^{\tilde{\chi}^0 \tilde{l}^*, L}$, which represents the left-handed coupling of the vertex neutralino-lepton-slepton ($\tilde{\chi}^0 - l - \tilde{l}^*$). $V_2^{L/R} = \Gamma_{j,a,c}^{\tilde{l} \tilde{\chi}^0 \tilde{l}, L/R}$, which represents the left(right)-handed coupling of the vertex anti lepton-neutralino-slepton ($\tilde{\chi}^0 - l - \tilde{l}^*$). $V_Z = \Gamma_{c,b}^{\tilde{l} \tilde{l}^* Z}$, which represents coupling of the vertex slepton-slepton-Z boson ($\tilde{l} - \tilde{l}^* - Z$). The concrete forms of the previous couplings are available in the Appendix A.

From eq. (3.5) the M parameter represents the neutralino mass $m_{\tilde{\chi}_a^0}$. The parameters C_0, C_{00}, C_1 and C_2 represent the standard three-point functions, their definition is given in the LoopTools package [56, 57]. Thus, they can be calculated by a specific Mathematica package called Package-X [58]. The arguments of C functions from figure 1(a) are $(0, m_Z^2, 0, m_{\tilde{\chi}_a^0}^2, m_{\tilde{l}_c}^2, m_{\tilde{l}_b}^2)$ where the external fermion masses have been set to zero.

The couplings corresponding to figure 1(b) are: $V_1^L = \Gamma_{a,i,b}^{\tilde{\chi}^+ l \nu^{I/R}, L}$, which represents the left-handed coupling of the vertex chargino-lepton-(CP-odd/CP-even) sneutrino ($\tilde{\chi}^+ - l - \nu^{I/R}$). $V_2^{L/R} = \Gamma_{j,a,c}^{l \tilde{\chi}^- \nu^{I/R}, L/R}$, which represents the left(right)-handed coupling of the vertex lepton-chargino-(CP-odd/CP-even) sneutrino ($l - \tilde{\chi}^- - \nu^{I/R}$). $V_Z = \Gamma_{b,c}^{\nu^I \nu^R Z} = -\Gamma_{c,b}^{\nu^I \nu^R Z}$, which represents coupling of the vertex CP-odd sneutrino - CP-even sneutrino - Z boson ($\nu^I - \nu^R - Z$).

From eq. (3.6) the M parameter represents the chargino mass $m_{\tilde{\chi}_a^\pm}$. The concrete forms of the above-mentioned couplings are available in the Appendix A. The arguments of C functions from figure 1(b) are $(0, m_Z^2, 0, m_{\tilde{\chi}_a^\pm}^2, m_{\nu_c^{R/I}}^2, m_{\nu_b^{I/R}}^2)$ where the external fermion masses have been set to zero. The contributions of figure 1(c,d) are:

$$A_1^{L(c,d)} = V_1^L V_2^R \left[V_Z^L C_0 m_1 m_2 - V_Z^R (B_0 - 2C_{00} + C_0) m_3^2 \right] \quad (3.7)$$

$$A_2^{L(c,d)} = 2V_1^L V_2^L \left[-V_Z^L C_1 m_1 + V_Z^R (C_0 + C_1 + C_2) m_2^2 \right] \quad (3.8)$$

$$\begin{aligned} A_1^R &= A_1^L(L \leftrightarrow R) \\ A_2^R &= A_2^L(L \leftrightarrow R) \end{aligned} \quad (3.9)$$

The couplings corresponding to figure 1(c) are: $V_1^{L/R} = \Gamma_{b,i,a}^{\tilde{\chi}^+ l \nu^{I/R}, L/R}$, $V_2^{R/L} = \Gamma_{j,c,a}^{\tilde{l} \tilde{\chi}^- \nu^{I/R}, R/L}$ and $V_Z^{L/R} = \Gamma_{c,b}^{\tilde{\chi}^+ \tilde{\chi}^- Z, L/R}$ which represents the coupling of the vertex chargino-chargino-Z boson ($\tilde{\chi}^+ - \tilde{\chi}^- - Z$). The m_1, m_2 and m_3 parameters represent the masses of chargino

and (CP-odd/CP-even) sneutrino ($m_{\tilde{\chi}_b^-}, m_{\tilde{\chi}_c^-}, m_{\nu_a^{I/R}}$) respectively. The concrete forms of the couplings are available in the Appendix A. The arguments of C functions from figure 1(c) are $(m_Z^2, 0, 0, m_{\tilde{\chi}_c^-}^2, m_{\tilde{\chi}_b^-}^2, m_{\nu_a^{I/R}}^2)$ where the external fermion masses have been set to zero. B_0 is a two-point function and its arguments are $(m_Z^2, m_{\tilde{\chi}_b^-}^2, m_{\tilde{\chi}_c^-}^2)$.

The couplings corresponding to figure 1(d) are: $V_1^L = \Gamma_{b,i,a}^{\tilde{\chi}^0 \tilde{l}^*, L}$, $V_2^{R/L} = \Gamma_{j,c,a}^{\tilde{l} \tilde{\chi}^0 \tilde{l}, R/L}$ and $V_Z^{L/R} = \Gamma_{c,b}^{\tilde{\chi}^0 \tilde{\chi}^0 Z, L/R}$ which represents coupling of the vertex neutralino-neutralino-Z boson ($\tilde{\chi}^0 - \tilde{\chi}^0 - Z$). The concrete forms of the couplings are available in the Appendix A. The m_1, m_2 and m_3 parameters represent the masses of neutralino and slepton ($m_{\tilde{\chi}_b^0}, m_{\tilde{\chi}_c^0}, m_{\tilde{l}_a}$) respectively. The arguments of C functions from figure 1(d) are $(m_Z^2, 0, 0, m_{\tilde{\chi}_c^0}^2, m_{\tilde{\chi}_b^0}^2, m_{\tilde{l}_a}^2)$ where the external fermion masses have been set to zero. The arguments of B function are $(m_Z^2, m_{\tilde{\chi}_b^0}^2, m_{\tilde{\chi}_c^0}^2)$.

The contributions of Feynman diagrams figure 1(e, f, g, h), here Z boson doesn't couple to a scalar particle therefore $A_2^{L/R} = 0$, can be written as follows:

$$A_1^L = \frac{V_Z^L}{m_1^2 - m_2^2} \left[-V_1^L V_2^R B_1 m_1^2 + V_1^R V_2^R B_0 m_1 m_3 - V_1^R V_2^L B_1 m_1 m_2 + V_1^L V_2^L B_0 m_3 m_2 \right] \quad (3.10)$$

$$A_1^R = A_1^L (L \leftrightarrow R) \quad (3.11)$$

The couplings corresponding to figure 1(e) are: $V_1^{L/R} = \Gamma_{a,i,b}^{\tilde{\chi}^0 \tilde{l}^*, L/R}$, $V_2^{R/L} = \Gamma_{a,i,b}^{\tilde{l} \tilde{\chi}^0 \tilde{l}, R/L}$ and $V_Z^L = \Gamma_{j,c}^{\tilde{l} Z, L}$ which represents the left-handed coupling of the vertex anti lepton-lepton-Z boson ($\tilde{l} - l - Z$). The m_1, m_2 and m_3 parameters represent the masses of leptons and neutralino ($m_{l_i}, m_{l_c}, m_{\tilde{\chi}_a^0}$), respectively. The arguments of B functions are $(m_{l_i}^2, m_{\tilde{\chi}_a^0}^2, m_{l_b}^2)$.

The couplings corresponding to figure 1(f) are: $V_1^{L/R} = \Gamma_{b,c,a}^{\tilde{\chi}^0 \tilde{l}^*, L/R}$, $V_2^{R/L} = \Gamma_{j,b,a}^{\tilde{l} \tilde{\chi}^0 \tilde{l}, R/L}$ and $V_Z^L = \Gamma_{c,i}^{\tilde{l} Z, L}$. Here m_1, m_2 and m_3 parameters represent the masses of ($m_{l_j}, m_{l_c}, m_{\tilde{\chi}_b^0}$) respectively. The arguments of B functions are $(m_{l_j}^2, m_{\tilde{\chi}_b^0}^2, m_{l_a}^2)$.

The couplings corresponding to figure 1(g) are: $V_1^{L/R} = \Gamma_{b,i,a}^{\tilde{\chi}^+ \tilde{l} \nu^{I/R}, L/R}$, $V_2^{R/L} = \Gamma_{c,b,a}^{\tilde{l} \tilde{\chi}^- \tilde{\nu}^{I/R}, R/L}$ and $V_Z^L = \Gamma_{j,c}^{\tilde{l} Z, L}$. Where m_1, m_2 and m_3 parameters represent the masses of leptons and chargino ($m_{l_i}, m_{l_c}, m_{\tilde{\chi}_b^-}$), respectively. The arguments of B functions are $(m_{l_i}^2, m_{\tilde{\chi}_b^-}^2, m_{\nu_a^{I/R}}^2)$.

The couplings corresponding to figure 1(h) are: $V_1^{L/R} = \Gamma_{a,c,b}^{\tilde{\chi}^+ \tilde{l} \nu^{I/R}, L/R}$, $V_2^{R/L} = \Gamma_{j,a,b}^{\tilde{l} \tilde{\chi}^- \tilde{\nu}^{I/R}, R/L}$ and $V_Z^L = \Gamma_{c,i}^{\tilde{l} Z, L}$. Where m_1, m_2 and m_3 parameters represent the masses of leptons and chargino ($m_{l_j}, m_{l_c}, m_{\tilde{\chi}_a^-}$), respectively. The arguments of B functions are $(m_{l_j}^2, m_{\tilde{\chi}_a^-}^2, m_{\nu_b^{I/R}}^2)$. The concrete forms of the couplings are available in the Appendix A.

4 Numerical results and discussion

In this section, the numerical results are implemented using the SARAH, SPheno and FlavorKit packages [43, 44, 59, 60]. SARAH package is a Mathematica package for building and analyzing SUSY and non-SUSY models, it creates source code for SPheno tool. SPheno

stands for S(upersymmetric) Pheno(menology). The code is written in Fortran-90 and it calculates the SUSY spectrum using low energy data and a user supplied high scale model as input like MSSM, Seesaw type-I (Seesaw type-II and Seesaw type-III), Next MSSM and the others models. Furthermore, the FlavorKit which is available within SARAH/Spheno can compute a wide range of flavor observables like LFV in Z boson, Higgs boson, and Tau lepton decays [45].

According to the MSSM-Seesaw type-II model, the final parameters in this study are: Y_T , M_T , f , $|n_e|$, $|n_\mu|$, $|n_\tau|$, $C_{\tau\mu}$, $C_{e\tau}$, $C_{e\mu}$, $m_{1/2}$, m_0 , A_0 , $\tan\beta$, $\text{sign}(\mu)$, λ_1 and λ_2 . In our calculations, the soft symmetry breaking terms are constrained by several theoretical and experimental conditions. Such as that the lightest supersymmetric particle of the considered model is the neutralino and the R-parity should be conserved. Furthermore, the supersymmetric particle masses (charginos, sleptons, sneutrinos and neutralinos) which are calculated with the SPheno package must be above the recent experimental mass limits [55], as shown in table 3.

Sparticle	Mass limits (GeV)
Sleptons	> 107
Sneutrinos	> 94
Neutralinos	> 46
Charginos	> 94

Table 3. Experimentally mass limits of supersymmetric particles [55].

The masses of the supersymmetric particles are related to both $m_{1/2}$ and m_0 , therefore we firstly determined their minimum values according to the previous conditions, so $m_{1/2}=200$ GeV and $m_0=550$ GeV. The parameters space for both $\tan\beta$ and A_0 is determined for obtaining numerical results by SPheno package without any error when running it. Errors typically occur for two main reasons: (i) Out of the values range of A_0 and $\tan(\beta)$, the gauge couplings become large at M_{GUT} due to large beta functions. Therefore, the perturbation theory will fail. (ii) Negative mass squares for the SUSY particles [41]. The values of input parameters in our study are shown in table 4.

Parameter	Values
m_0 (GeV)	[550,1550]
$m_{1/2}$ (GeV)	[200,400]
A_0 (GeV)	[-850,900]
$\tan\beta$	[5,35]
$\cos(\theta_{ij})$	[0.087,0.87]

Table 4. Values range of input parameters considered in this study.

From eqs. (2.23), (2.30), (2.32) and (2.34), we can estimate both the values of triplet Yukawa matrix elements (Yukawa couplings) and the scalar triplet mass M_T according to the mass limit condition for the light neutrino which is estimated to be < 0.8 eV at

low energy scale [9]. We can guess the Yukawa matrix elements for any fixed value of the neutrino mass as a function of the triplet mass for any fixed value of the Yukawa couplings. This guess will not provide the correct values of the Yukawa couplings because the neutrino masses are measured at low energy scale, in order to calculate the neutrino masses (m_ν) from eq. (2.23) we should insert the parameters M_T and Y_T at high energy scale. However, we can use our guess to run the RGEs numerically to obtain the exact light neutrino masses for these input parameters at low energy scale. The difference between these results could be obtained numerically, then input numbers could be minimized in a simple iterative procedure until the convergence is achieved. We can reach this convergence in several steps as long as the Yukawa matrix elements satisfy this condition $|(Y_T)_{ij}| < 1$ [41].

In this work, the sizable values for the triplet Yukawa couplings are considered, taking into account that they should still within the perturbative regime. Thus, the constraint on the allowed maximum entries values of the Yukawa matrix is chosen to be: $|(Y_T)_{ij}|^2 < 4\pi$ [51], so we get $M_T \geq 5 \times 10^{13}$ GeV and $\cos(\theta_{ij}) \leq 0.87$. We fixed $\lambda_1 = \lambda_2 = 0.5$ and $\text{sign}(\mu) > 0$ as in Ref [10] for all numerical calculations. From eqs. (2.30), (2.32) and (2.34) we have three scenarios of the Yukawa coupling matrix for Z boson LFV decays, we set the values of $|n_e|$, $|n_\mu|$ and $|n_\tau|$ as shown in table 5. The energy scale of GUT is fixed to $M_{GUT} = 2.00 \times 10^{16}$ GeV. While, the supersymmetric breaking scale is fixed to $M_{SUSY} = 10^3$ GeV [38]. We will study $\text{BR}(Z \rightarrow l_i l_j)$ with(without) applying the constraints due to non-observation of $(l_i \rightarrow l_j \gamma)$.

Scenario	$C_{\tau\mu}$	$C_{e\tau}$	$C_{e\mu}$	$ n_e $	$ n_\mu $	$ n_\tau $	Example
MT	$C_{\tau\mu}$	0	0	0.1	1	1	$Y_T = f \begin{pmatrix} 0.1 & 0 & 0 \\ 0 & 1 & C_{\tau\mu} \\ 0 & 0 & \sqrt{1 - C_{\tau\mu}^2} \end{pmatrix}$
ET	0	$C_{e\tau}$	0	1	0.1	1	$Y_T = f \begin{pmatrix} 1 & 0 & C_{e\tau} \\ 0 & 0.1 & 0 \\ 0 & 0 & \sqrt{1 - C_{e\tau}^2} \end{pmatrix}$
EM	0	0	$C_{e\mu}$	1	1	0.1	$Y_T = f \begin{pmatrix} \sqrt{1 - C_{e\mu}^2} & 0 & 0 \\ C_{e\mu} & 1 & 0 \\ 0 & 0 & 0.1 \end{pmatrix}$

Table 5. Yukawa matrix scenarios for numerical calculations of $\text{BR}(Z \rightarrow l_i l_j)$.

4.1 $\text{BR}(Z \rightarrow l_i l_j)$ without constraints on $(l_i \rightarrow l_j \gamma)$

4.1.1 $\text{BR}(Z \rightarrow l_i l_j)$ as a function of A_0 , $\tan(\beta)$, M_T and $\cos(\theta_{ij})$ parameters

From eq. (2.25) A_0 and $\cos(\theta_{ij})$ parameters present in non-diagonal elements of the left sleptons mass matrix and tri-linear coupling terms (RGEs). Effects of $\cos(\theta_{ij})$ in the numerical results arise from the product $Y_T^t Y_T$. The parameters Δm_L^2 and ΔT_L^2 are proportional to A_0^2 , A_0 and $(Y_T^t Y_T)_{ij}$. Here $(Y_T^t Y_T)_{ij} = f^2 n_i n_j \cos(\theta_{ij})$ where i, j indicate to the neutrino

generation. The Y_T matrix and M_T parameter are also related to Weinberg operator which is in turn related to the mass matrix of CP-even and CP-odd sneutrino as in eqs. (2.8) and (2.10), thus the contributions from sneutrino-chargino can be influenced by elements of the Y_T matrix and the values of the triplet mass M_T . The variation of $\text{BR}(Z \rightarrow l_i l_j)$ as a function of $\cos(\theta_{ij})$ also as a contour of A_0 and $\tan\beta$ are studied as shown in figure 2.

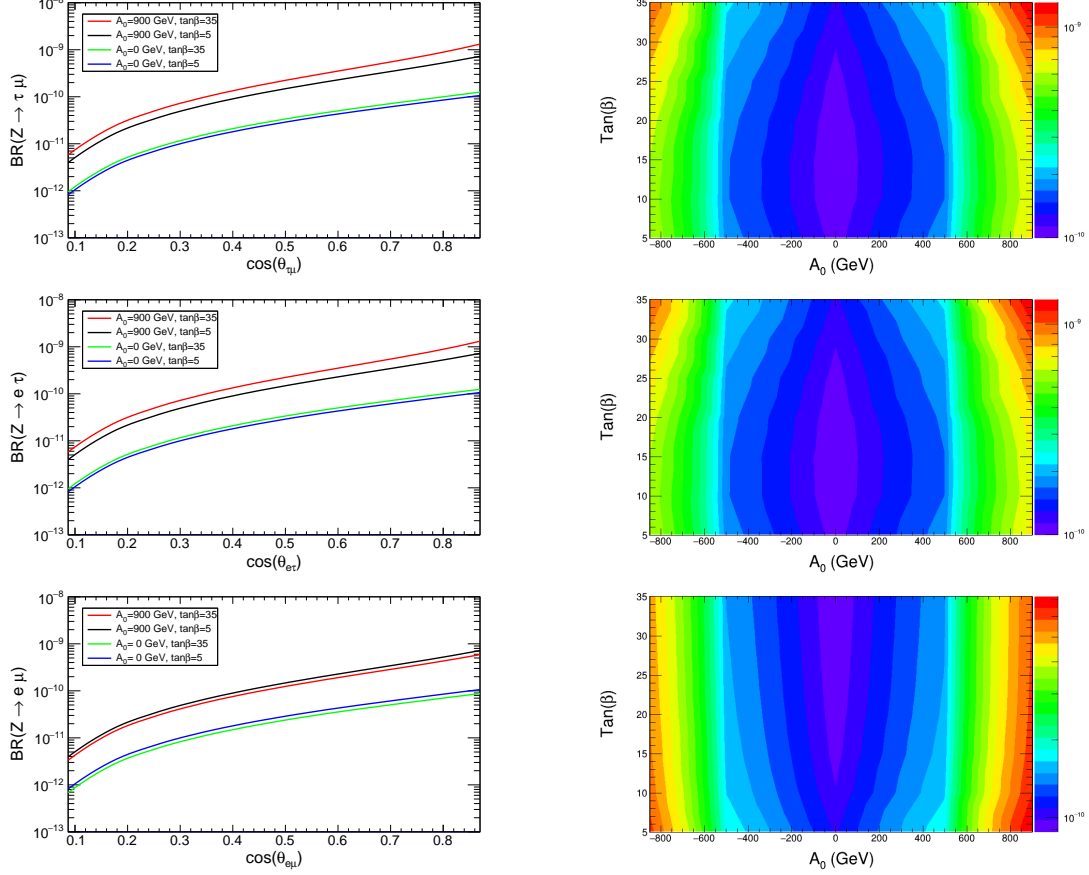


Figure 2. $\text{BR}(Z \rightarrow l_i l_j)$ as a function of $\cos(\theta_{ij})$ at $A_0 = 0, 900$ GeV and $\tan\beta=5, 35$ (left). $\text{BR}(Z \rightarrow l_i l_j)$ as a contour in the A_0 and $\tan\beta$ plane at $\cos(\theta_{ij})=0.87$ (Right). For all above plots we set $m_{1/2} = 200$ GeV, $m_0 = 550$ GeV, $f = 1$ and $M_T = 5 \times 10^{13}$ GeV.

Figure 2 shows in the left side that BRs of Z decays increase as the values of $\cos(\theta_{ij})$ variate from 0.087 to 0.87 for these two cases $A_0 = 0, 900$ GeV and $\tan\beta=5, 35$. For $A_0 = 900$ GeV and $\tan\beta=35$ we get the best value of $\text{BR}(Z \rightarrow \tau l)$ (red line). While the best value of $\text{BR}(Z \rightarrow e\mu)$ are at $A_0 = 900$ GeV and $\tan\beta=5$ (black line). Furthermore, we notice that $\text{BR}(Z \rightarrow e\mu) = \text{BR}(Z \rightarrow \tau l)$ at $A_0 = 0$ GeV and $\tan\beta=5, 35$ (green and blue lines).

Figure 2 shows in the right side the $\text{BR}(Z \rightarrow l_i l_j)$ as a contour of A_0 and $\tan\beta$ at $\cos(\theta_{ij})=0.87$. It is obvious that the values of $\text{BR}(Z \rightarrow l_i l_j)$ increase by increasing the absolute values of A_0 at any fixed value of $\tan\beta$. This means that the sign of A_0 has no considerable effect on the prediction of BRs ZLFV decays. However, the sign of A_0 is still

relevant to the precise predictions. It is also clear that the variation of $\text{BR}(Z \rightarrow l_i l_j)$ is very small when $5 \leq \tan\beta \leq 35$ at a fixed value of A_0 . This means that the presence of A_0 and $\cos(\theta_{ij})$ in the RGEs increase the branching ratios of $Z \rightarrow l_i l_j$. While the dependence of ZLFV decays on $\tan\beta$ is weak so that $\tan\beta$ is not embedded in the RGEs. Furthermore, we notice that $5 \times 10^{-10} \leq \text{BR}(Z \rightarrow \mu e) \leq 7 \times 10^{-10}$ when $5 \leq \tan\beta \leq 35$ at $A_0 = 900$ and -850 GeV. For the other two decay channels it is obvious that $\text{BR}(Z \rightarrow \tau e) = \text{BR}(Z \rightarrow \tau \mu)$ at $5 \leq \tan\beta \leq 35$ and $-850 \leq A_0 \leq 900$ GeV. Hence, the best value of $\text{BR}(Z \rightarrow \tau l)$ is in the order of $\sim 1 \times 10^{-9}$ at $\tan\beta = 35$ and $A_0 = 900$ GeV (red region). Thus, we fix $\tan\beta = 35$ and $A_0 = 900$ GeV for the next calculations.

We plot $\text{BR}(Z \rightarrow l_i l_j)$ versus strength of the neutrino Yukawa coupling (f) for these two values $M_T = 5 \times 10^{+13} / 5 \times 10^{+14}$ GeV as shown in figure 3.

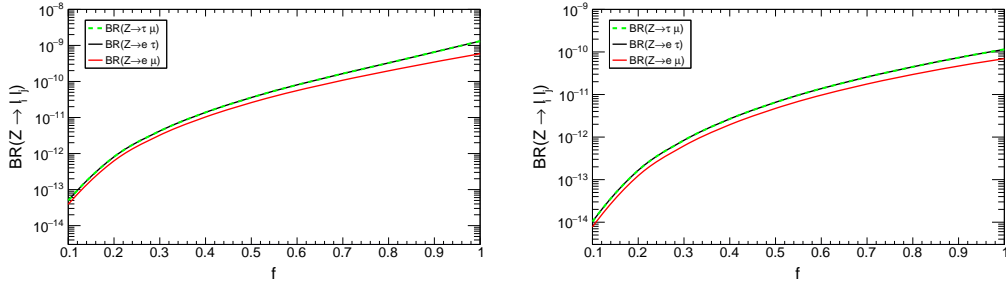


Figure 3. $\text{BR}(Z \rightarrow l_i l_j)$ as a function of strength of the neutrino Yukawa coupling (f) at the two values $M_T = 5 \times 10^{+13}$ (left), and $5 \times 10^{+14}$ GeV (right). $\text{BR}(Z \rightarrow \mu \tau)$ in dashed-green line, $\text{BR}(Z \rightarrow e \tau)$ in black one and $\text{BR}(Z \rightarrow e \mu)$ in red one. Where the other input parameter are fixed as $m_0 = 550$ GeV, $m_{1/2} = 200$ GeV, $A_0 = 900$ GeV, $\tan\beta=35$ and $\cos(\theta_{ij})=0.87$.

Here the red line denotes $\text{BR}(Z \rightarrow e \mu)$, the black one denotes $\text{BR}(Z \rightarrow e \tau)$ and the dashed-green one denotes $\text{BR}(Z \rightarrow \tau \mu)$. The values of BRs of ZLFV decays increase by increasing the f parameter values. The values of the BRs are better at $M_T = 5 \times 10^{+13}$ than at $M_T = 5 \times 10^{+14}$. At $M_T = 5 \times 10^{+13}$ GeV the range of $\text{BR}(Z \rightarrow e \mu)$ is $[4 \times 10^{-14}, 6 \times 10^{-10}]$ and for $\text{BR}(Z \rightarrow \tau l)$ is $[5 \times 10^{-14}, 1.3 \times 10^{-9}]$. While At $M_T = 5 \times 10^{+14}$ GeV the range of $\text{BR}(Z \rightarrow e \mu)$ is $[7 \times 10^{-15}, 7 \times 10^{-11}]$ and for $\text{BR}(Z \rightarrow \tau l)$ is $[1 \times 10^{-14}, 1.1 \times 10^{-10}]$.

4.1.2 $\text{BR}(Z \rightarrow l_i l_j)$ as a contour of m_0 and $m_{1/2}$ parameters

In this case, the m_0 parameter is related to the soft breaking slepton mass terms $m_{\tilde{L}}$ and the mass matrices of sleptons and CP-odd(CP-even) sneutrinos. The $m_{1/2}$ parameter is related to the soft breaking gaugino mass terms and the mass matrices of both neutralino and chargino. So that both m_0 and $m_{1/2}$ can induce the contributions from neutralino-slepton and chargino-sneutrino. We plot $\text{BR}(Z \rightarrow l_i l_j)$ as a contour in the m_0 and $m_{1/2}$ plane as shown in figure 4. In this case the other input parameters are fixed as follows: $A_0 = 900$ GeV, $\tan \beta = 35$, $\cos(\theta_{ij}) = 0.87$ and $M_T = 5 \times 10^{13}$ GeV.

We notice that the $\text{BR}(Z \rightarrow l_i l_j)$ decreases by increasing both m_0 and $m_{1/2}$. This means that ZLFV decays depend strongly on m_0 and $m_{1/2}$. The best values of BRs are

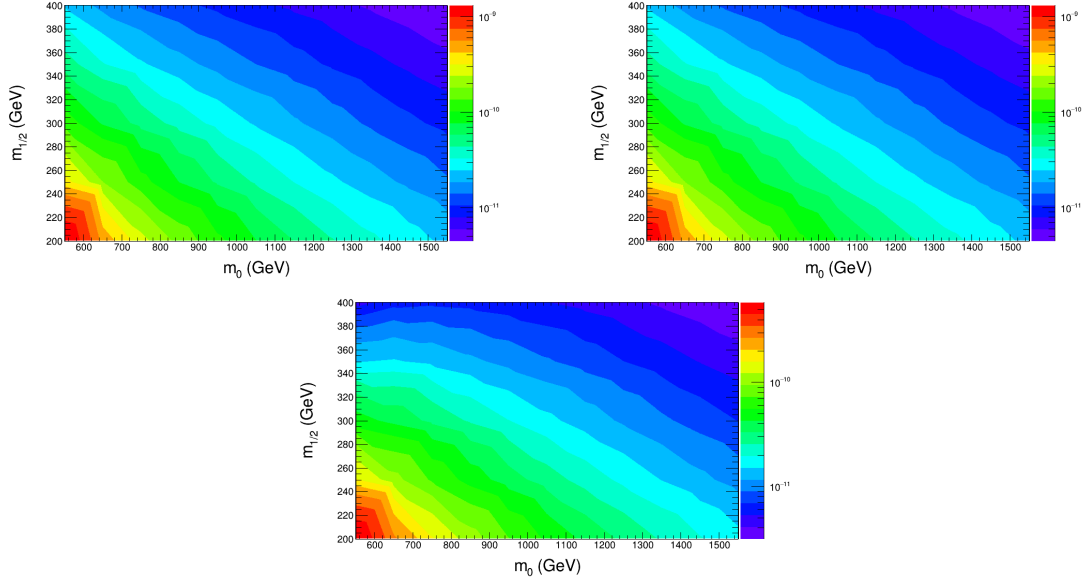


Figure 4. $\text{BR}(Z \rightarrow l_i l_j)$ as a contour of m_0 and $m_{1/2}$. $\text{BR}(Z \rightarrow \mu\tau)$ top-left, $\text{BR}(Z \rightarrow e\tau)$ top-right and $\text{BR}(Z \rightarrow e\mu)$ bottom. The best values of $\text{BR}(Z \rightarrow l_i l_j)$ for all decay channels are in red region.

at $m_0 = [550, 590]$ GeV and $m_{1/2} = [200, 215]$ GeV (red region). Thus, ZLFV decays can occur at the low mass limit of SUSY particles where their masses increase by increasing of m_0 and $m_{1/2}$. Moreover, contributions of non-diagonal elements of sleptons mass matrix in ZLFV decays decrease by increasing of m_0 . The best value of $\text{BR}(Z \rightarrow \tau l)$ is in the order of $\sim 1 \times 10^{-9}$ while for $\text{BR}(Z \rightarrow e \mu)$ it is in the order of $\sim 6 \times 10^{-10}$.

Regarding the Yukawa couplings and the mass limits of SUSY particles, the branching ratios for $(l_i \rightarrow l_j \gamma)$ decays are quite large so that they do not respect the experimental limits as shown in table 6. Hence, the previous plots show the maximum values which $\text{BR}(Z \rightarrow l_i l_j)$ can reach in the MSSM-Seesaw type-II model without applying constraints on these decays.

4.2 $\text{BR}(Z \rightarrow l_i l_j)$ with constraints on $(l_i \rightarrow l_j \gamma)$

In this section, we study the variation of $\text{BR}(Z \rightarrow l_i l_j)$ after applying constraints on $\text{Br}(l_i \rightarrow l_j \gamma)$. The $(l_i \rightarrow l_j \gamma)$ decays are not observed in any experiment. Hence, the branching ratios for these decays are constrained as shown in table 6.

Decay	Upper Limit	Experiment
$BR(\tau \rightarrow \mu \gamma)$	4.2×10^{-8} [61]	Belle
$BR(\tau \rightarrow e \gamma)$	5.6×10^{-8} [61]	Belle
$BR(\mu \rightarrow e \gamma)$	4.2×10^{-13} [62]	MEG

Table 6. Experimental upper limits of lepton flavor violating of radiative two body decays $(l_i \rightarrow l_j \gamma)$.

In supersymmetry, the source of the LFV processes can be non-diagonal elements in the left slepton mass matrix. Therefore, in the mass insertion method (MI) with leading-logarithm approximation, the branching ratios of $(l_i \rightarrow l_j \gamma)$ decays can be approximated as follows [37, 41]:

$$BR(l_i \rightarrow l_j \gamma) \propto \alpha^3 m_{l_i}^5 \frac{|\Delta m_{Lij}^2|^2}{\tilde{m}^8} \tan^2(\beta) \quad (4.1)$$

Where α is the electroweak coupling constant, m_{l_i} is the mass of lepton i and \tilde{m} is the average of SUSY masses that is involved in loops. From the above-mentioned study (section 4.1) the branching ratios for $(l_i \rightarrow l_j \gamma)$ decays are quite large. However, this does not completely exclude the MSSM-Seesaw type-II model since there are certain parameter regions where cancellations between different contributions can occur. From eqs. (2.25) and (4.1), we notice that $BR(l_i \rightarrow l_j \gamma)$ are mainly related to the SUSY mass scale and elements of non-diagonal left slepton mass matrix. Non-diagonal elements are almost completely governed by the choice of the soft SUSY breaking parameters in the heavy seesaw sector. Furthermore, $BR(l_i \rightarrow l_j \gamma)$ is proportional to the square of $\tan\beta$ which leads to larger LFV branching ratios. Therefore, we fixed $A_0 = 0$ GeV (to exclude tri-linear couplings) and $\tan\beta=5$ for all our calculations. We fixed also $m_0 = 550$ GeV and $m_{1/2} = 200$ GeV by considering conditions of the mass limits of SUSY particles as shown in table 3. We utilize the $(l_i \rightarrow l_j \gamma)$ LFV decays to constrain the f parameter while the values of the Y_T matrix are fixed as shown in table 5. Sparticles mediated diagrams (sleptons, sneutrinos, neutralinos and charginos) for the $(l_i \rightarrow l_j \gamma)$ LFV decays in the MSSM-Seesaw type-II model are shown in figure 5.

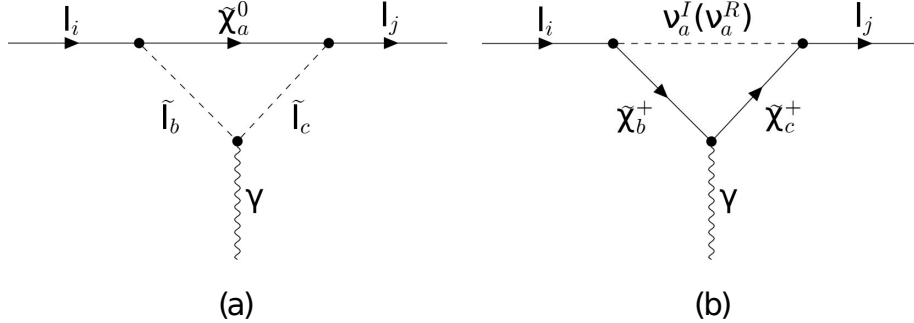


Figure 5. One loop Feynman diagrams contributing to $BR(l_i \rightarrow l_j \gamma)$ in the MSSM-Seesaw type-II model.

The off-shell amplitude for $(l_i \rightarrow l_j \gamma)$ is given by [45, 63]:

$$M = e\epsilon^{\alpha*} \bar{u}_i(p-q) [q^2 \gamma_\alpha (K_1^L P_L + K_1^R P_R) + m_{l_i} i \sigma_{\alpha\beta} q^\beta (K_2^L P_L + K_2^R P_R)] u_j(p) \quad (4.2)$$

Here q represents the momentum of photon. e is the electric charge, ϵ^α is the polarization vector of photon, u_i and u_j represent the wave function for anti-lepton/lepton and p

is momentum of the lepton li . In the limit $q \rightarrow 0$, the analytic expression of the branching ratio of the $(l_i \rightarrow l_j \gamma)$ decays is:

$$BR(l_i \rightarrow l_j \gamma) = \alpha \frac{m_{li}^5}{\Gamma_{li}} (|K_2^L|^2 + |K_2^R|^2) \quad (4.3)$$

Where α is the fine structure constant and Γ_{li} is the total decay width of l_i . $K_2^{L/R}$ are the combinations of the coefficients which correspond to Feynman diagrams as in figure 5 and could be written as:

$$K_2^{L/R} = K_{2a}^{L/R} + K_{2b}^{L/R} \quad (4.4)$$

Here the contributions from neutralino-slepton loops are shown in figure 5(a). While the contributions from chargino-sneutrino loops are shown in figure 5(b). The contribution of figure 5(a) is given by:

$$K_2^L = 2V_\gamma [V_1^L V_2^R (C_2 + C_{12} + C_{11}) m_{e_i} + V_1^R V_2^L (C_1 + C_{12} + C_{11}) m_{e_j} - V_1^R V_2^R (C_0 + C_1 + C_2) m_{\tilde{\chi}_a^0}] \quad (4.5)$$

$$K_2^R = K_2^L (L \leftrightarrow R) \quad (4.6)$$

The couplings corresponding to figure 5(a) are: $V_\gamma = \Gamma_{c,b}^{\tilde{l} \tilde{l}^* \gamma}$ which represents the coupling of vertex slepton-slepton-gamma, $V_1^{(L/R)} = \Gamma_{i,a,b}^{\tilde{l} \tilde{\chi}^0 \tilde{l}, (L/R)}$ which represents the left(right)-handed coupling of vertex anti lepton-neutralino-slepton, and $V_2^{(L/R)} = \Gamma_{a,j,c}^{\tilde{\chi}^0 \tilde{l}^*, (L/R)}$ which represents the left(right)-handed coupling of vertex neutralino-lepton-slepton. The concrete forms of couplings are included in the Appendix A. While $C_0, C_{00}, C_1, C_2, C_{11}, C_{12}$ are the standard three-point functions with their definition given in the LoopTools program [56, 57], and it can be calculated by the Mathematica package Package-X [58]. The arguments of the C functions with vanishing external momenta of figure 5(a) are $(m_{\tilde{\chi}_a^0}^2, m_{\tilde{l}_c}^2, m_{\tilde{l}_b}^2)$. The contribution of figure 5(b) is given by:

$$K_2^L = -2(V_\gamma^L)^* V_1^L V_2^R C_{12} m_{e_i} + 2(V_\gamma^R)^* V_1^R V_2^L (C_2 + C_{12} + C_{22}) m_{e_j} + 2(V_\gamma^L)^* V_1^R V_2^R C_1 m_{\tilde{\chi}_b^-} - 2(V_\gamma^R)^* V_1^R V_2^R (C_0 + C_1 + C_2) m_{\tilde{\chi}_c^-} \quad (4.7)$$

$$K_2^R = K_2^L (L \leftrightarrow R) \quad (4.8)$$

The couplings corresponding to figure 5(b) are $V_\gamma^{(L/R)} = \Gamma_{b,c}^{\tilde{\chi}^+ \tilde{\chi}^- \gamma, (L/R)}$ which represents the left(right)-handed coupling of vertex chargino-chargino-gamma, $V_1^{(L/R)} = \Gamma_{i,b,a}^{\tilde{l} \tilde{\chi}^- \nu^I, (L/R)}$ which represents the left(right)-handed coupling of vertex anti lepton-chargino-CP-odd sneutrino, and $V_2^{(L/R)} = \Gamma_{c,j,a}^{\tilde{\chi}^+ \nu^I, (L/R)}$ which represents the left(right)-handed coupling

of vertex chargino-lepton- CP-even sneutrino. The concrete forms of couplings are included in the Appendix A. While $C_0, C_1, C_2, C_{12}, C_{22}$ are the standard three-point functions. The arguments of C functions with vanishing external momenta from figure 5(b) are $(m_{\tilde{\chi}_c^-}^2, m_{\tilde{\chi}_b^-}^2, m_{\nu_a^I}^2)$. For the CP-even sneutrino couplings we replace ν^I with ν^R in the last two vertices $V_1^{(L/R)}, V_2^{(L/R)}$ and the arguments of C functions.

After studying the analytical expression of $\text{BR}(l_i \rightarrow l_j \gamma)$, we start the numerical discussion with μ decays since their limits are strongest in this case. By taking $m_0 = 550$ GeV, $m_{1/2} = 200$ GeV, $\tan\beta=5$, $M_T = 5 \times 10^{13}$ GeV and $A_0 = 0$ GeV. We plot both $\text{BR}(\mu \rightarrow e \gamma)$ and $\text{BR}(Z \rightarrow e \mu)$ versus the f parameter as shown in figure 6 at $\cos(\theta_{e\mu}) = 0.87, 0.57$ and 0.17 . The horizontal dotted line is the $\text{BR}(\mu \rightarrow e \gamma)$ current experimental limit as shown in table 6.

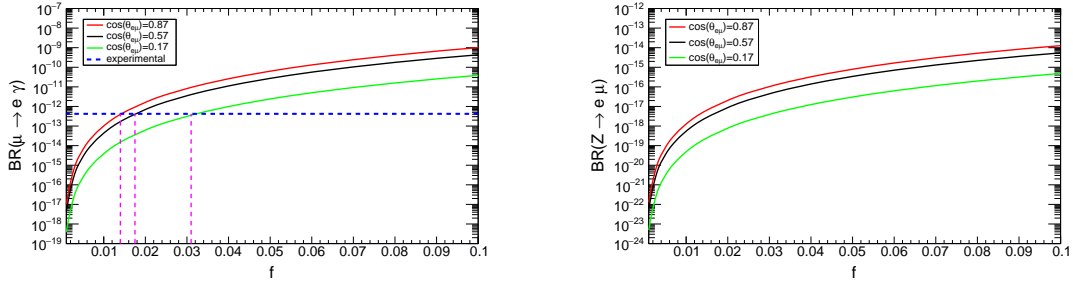


Figure 6. $\text{BR}(\mu \rightarrow e \gamma)$ versus f (left), $\text{BR}(Z \rightarrow e \mu)$ versus f (right). For these two plots we set $\cos(\theta_{e\mu})=0.87$ in red line, $\cos(\theta_{e\mu})=0.57$ in black one and $\cos(\theta_{e\mu})=0.17$ in green one.

It is obvious that both $\text{BR}(\mu \rightarrow e \gamma)$ and $\text{BR}(Z \rightarrow e \mu)$ increase as the f parameter varies from 0.001 to 0.1. The prediction on $\text{BR}(\mu \rightarrow e \gamma)$ exceeds the current experimental limit at $f = 0.014, 0.0175$ and 0.031 in red, black and green line respectively. So in this case the $\text{BR}(Z \rightarrow e \mu)$ is 4.7×10^{-18} , 5.10×10^{-18} and 5.09×10^{-18} at $f = 0.014$ ($\cos(\theta_{e\mu})=0.87$), 0.0175 ($\cos(\theta_{e\mu})=0.57$) and 0.031 ($\cos(\theta_{e\mu})=0.17$) respectively. Thus, under constraints of $\text{BR}(\mu \rightarrow e \gamma)$ the value of $\text{BR}(Z \rightarrow e \mu)$ is about 5×10^{-18} . This predicted value is eleven orders of magnitude below the current experimental limit and eight orders below the sensitivity of future colliders as shown in table 1.

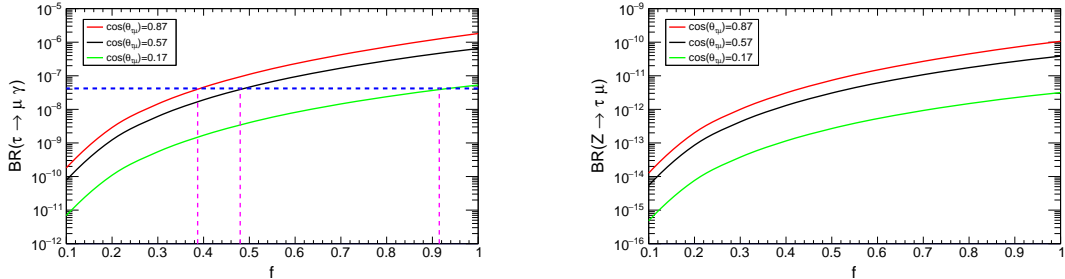


Figure 7. (left) $\text{BR}(\tau \rightarrow \mu \gamma)$ versus f , (right) $\text{BR}(Z \rightarrow \tau \mu)$ versus f . For these two plots we set $\cos(\theta_{\tau\mu})=0.87$ in red line, $\cos(\theta_{\tau\mu})=0.57$ in black one and $\cos(\theta_{\tau\mu})=0.17$ in green one.

In figure 7, we plot both $\text{BR}(\tau \rightarrow \mu\gamma)$ and $\text{BR}(Z \rightarrow \tau\mu)$ versus the f parameter at $\cos(\theta_{\tau\mu}) = 0.87, 0.57$ and 0.17 . The horizontal dotted line is the $\text{BR}(\tau \rightarrow \mu\gamma)$ current experimental limit as shown in table 6. It is clear that both $\text{BR}(\tau \rightarrow \mu\gamma)$ and $\text{BR}(Z \rightarrow \tau\mu)$ increase as the f parameter varies from 0.1 to 1. The prediction on $\text{BR}(\tau \rightarrow \mu\gamma)$ exceeds the current experimental limit at $f = 0.387, 0.48, 0.915$ in red line, black and green one respectively. So, in this case the $\text{BR}(Z \rightarrow \tau\mu)$ is 2.8×10^{-12} , 2.5×10^{-12} and 2.1×10^{-12} at $f = 0.387$ ($\cos(\theta_{\tau\mu})=0.87$), 0.48 ($\cos(\theta_{\tau\mu})=0.57$) and 0.915 ($\cos(\theta_{\tau\mu})=0.17$) respectively. Thus, under the constraints on the $(\tau \rightarrow \mu\gamma)$ decay the value of $\text{BR}(Z \rightarrow \tau\mu)$ is about 2×10^{-12} . This predicted value is six orders of magnitude below the current experimental limit and four orders below the sensitivity of future colliders as shown in table 1.

In figure 8, we plot both $\text{BR}(\tau \rightarrow e\gamma)$ and $\text{BR}(Z \rightarrow e\tau)$ versus the f parameter at $\cos(\theta_{e\tau}) = 0.87, 0.57$ and 0.17 . The horizontal dotted line is the $\text{BR}(\tau \rightarrow e\gamma)$ current experimental limit as shown in table 6.

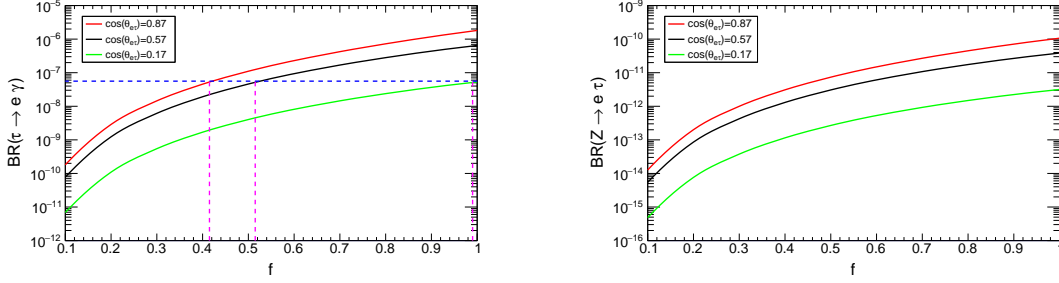


Figure 8. $\text{BR}(\tau \rightarrow e\gamma)$ versus f (left), $\text{BR}(Z \rightarrow e\tau)$ versus f (right). For these two plots we set $\cos(\theta_{e\tau})=0.87$ in red line, $\cos(\theta_{e\tau})=0.57$ in black one and $\cos(\theta_{e\tau})=0.17$ in green one.

We can see that both $\text{BR}(\tau \rightarrow e\gamma)$ and $\text{BR}(Z \rightarrow e\tau)$ increase as the f parameter varies from 0.1 to 1. The prediction of $\text{BR}(\tau \rightarrow e\gamma)$ exceeds the current experimental limit at $f = 0.415, 0.515, 0.99$ in red line, black and green one respectively. So, in this case the $\text{BR}(Z \rightarrow e\tau)$ is 3.56×10^{-12} , 3.47×10^{-12} and 3.1×10^{-12} at $f = 0.415$ ($\cos(\theta_{e\tau})=0.87$), 0.515 ($\cos(\theta_{e\tau})=0.57$) and 0.99 ($\cos(\theta_{e\tau})=0.17$) respectively. Thus, under the constraints of the $(\tau \rightarrow e\gamma)$ decay, the value of $\text{BR}(Z \rightarrow e\tau)$ is about 3×10^{-12} . This predicted value is six orders of magnitude below the current experimental limit and four orders below the sensitivity of future colliders as shown in table 1.

The obtained numerical results indicate that when the $\cos(\theta_{ij})$ parameter increase the value of the f parameter is constrained to be small and the predicted values of $\text{BR}(Z \rightarrow l_i l_j)$ are approximately equal for these values of $\cos(\theta_{ij})=0.87, 0.57$ and 0.17 .

The two parameters m_0 and $m_{1/2}$ are associated with the soft breaking slepton mass matrices and the soft breaking gaugino masses at GUT scale. Theses parameters contribute to the mass of sparticles at low energy by RGEs. The mass of sleptons, sneutrinos, neutralinos and charginos contribute to the LFV by one-loop functions in the electroweak interaction basis. The m_0 and $m_{1/2}$ parameters also contribute in the non-diagonal elements of the slepton matrices so it have an effect on the LFV. The variation of $\text{BR}(Z \rightarrow l_i l_j)$ as a function of m_0 at $m_{1/2}=200, 600$ and 1000 GeV are shown in figure 9.

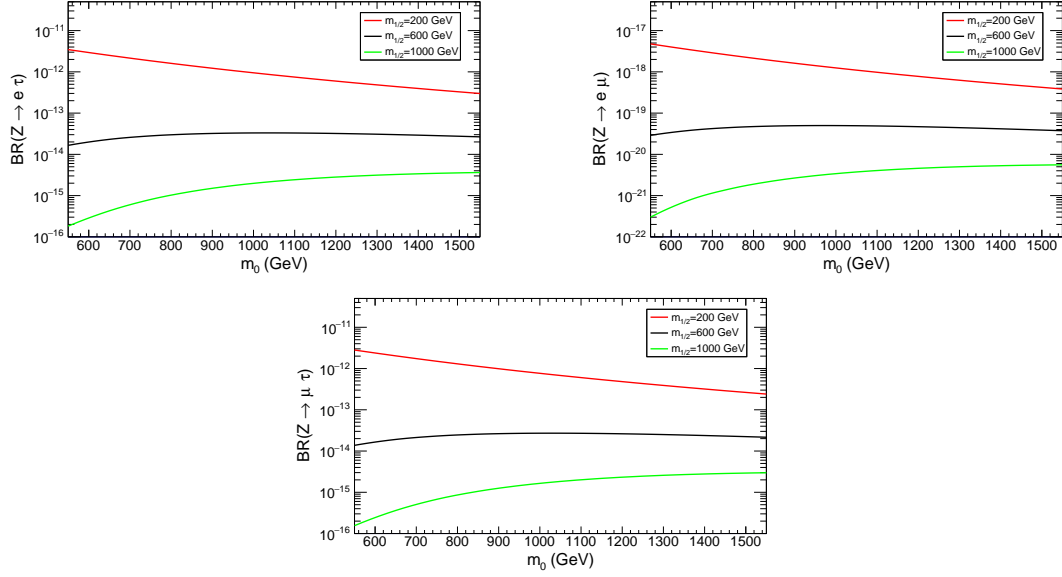


Figure 9. $\text{BR}(Z \rightarrow l_i l_j)$ as a function of m_0 at $m_{1/2}=200, 600$ and 1000 GeV. $m_{1/2}=200, 600$ and 1000 GeV. Where $f=0.387$ for $\text{BR}(Z \rightarrow \mu\tau)$, $f=0.415$ for $\text{BR}(Z \rightarrow e\tau)$ and $f=0.014$ for $\text{BR}(Z \rightarrow e\mu)$ at $\cos(\theta_{ij})=0.87$.

In this case we set $\cos(\theta_{ij})=0.87$ and $f=0.387$ for $\text{BR}(Z \rightarrow \mu\tau)$, $f=0.415$ for $\text{BR}(Z \rightarrow e\tau)$ and $f=0.014$ for $\text{BR}(Z \rightarrow e\mu)$. The numerical results show that when $m_{1/2}$ increases the BRs of Z decays decrease. Also, when m_0 varies from 550 to 1550 GeV the BRs of Z decays have a small increase at $m_{1/2}=600, 1000$ GeV respectively. While the BRs of Z decays have a small decrease at $m_{1/2}=200$ GeV when m_0 increases. This indicates that the large values of $m_{1/2}$ suppress the LFV in Z decays. Furthermore, under constraints of the $(l_i \rightarrow l_j \gamma)$ decays and $\cos(\theta_{ij})=0.87$ the numerical results show that $\text{BR}(Z \rightarrow e\mu)$ falls within $[3 \times 10^{-22}, 5 \times 10^{-18}]$ while $\text{BR}(Z \rightarrow e\tau)$ falls within $[1.8 \times 10^{-16}, 3.46 \times 10^{-12}]$ and $\text{BR}(Z \rightarrow \mu\tau)$ falls within $[1.5 \times 10^{-16}, 2.8 \times 10^{-12}]$.

5 Conclusions

The lepton flavor violation (LFV) of the Z boson decays ($Z \rightarrow l_i l_j$) in the CMSSM-Seesaw type-II model is studied in this article. In the supersymmetric models (SUYS), the type-II Seesaw mechanism can be realized by adding a scalar triplet superfield. After deriving the analytical expressions for the branching ratios (BRs) of both the Z boson and the radiative two body ($l_i \rightarrow l_j \gamma$) decays, we have predicted the BRs values of the Z boson LFV decays in the studied model. The numerical study has been performed by implementing the following constraints: The R-parity is conserved, fit to small neutrino masses and neutralino is the lightest supersymmetric particle of the considered model. Furthermore, we take into account that the sparticles (charginos, sleptons, sneutrinos and neutralinos) masses should be above the recent experimental mass limits. We set also the constraints on $\text{BR}(l_i \rightarrow l_j \gamma)$ and perturbativity limits on the parameters of this model. For investigation of the small

masses of the left-handed neutrinos, the mass of a scalar triplet M_T should be in the order of $\geq 5 \times 10^{13}$ GeV. After satisfying all constraints on the model parameters with(without) constraints on the $l_i \rightarrow l_j \gamma$ decays, the maximum values of BRs of the Z boson LFV decays are summarized in table 7.

Z Decays	Our results ¹	Our results ²	LHC(90%)	FCC-ee/CEPC
$\text{BR}(Z \rightarrow \mu\tau)$	1.00×10^{-9}	2.8×10^{-12}	7.20×10^{-6}	10^{-9}
$\text{BR}(Z \rightarrow e\tau)$	1.00×10^{-9}	3.46×10^{-12}	7.00×10^{-6}	10^{-9}
$\text{BR}(Z \rightarrow e\mu)$	6.00×10^{-10}	5.00×10^{-18}	2.62×10^{-7}	$10^{-8} - 10^{-10}$

Table 7. Values of upper limits of BRs for ZLFV decays. This study prediction, ATLAS experiment and FCC-ee/CEPC expectation. The statements Our results1(Our results2) means without(with) constraints on the $l_i \rightarrow l_j \gamma$ decays.

These values are out of the experimental upper limits for the LHC, while they are in coincidence with the sensitivity of the future colliders (FCC-ee/CEPC) for the scenario without constraints on the $l_i \rightarrow l_j \gamma$ decays as shown in table 7. On the other hand, for the scenario with constraints on the $l_i \rightarrow l_j \gamma$ decays, the above-mentioned results on the BRs of the Z boson LFV decays get an additional suppression of about 10^{-3} for $\text{BR}(Z \rightarrow l\tau)$ and 10^{-8} for $\text{BR}(Z \rightarrow e\mu)$ when they are compared to the sensitivity of the future colliders (FCC-ee/CEPC). Hence, the branching ratios predictions are several orders below the recent experimental limits for both scenarios, which give a very low possibility to observe the LFV decays of Z boson in the future collider experiments. Finally according to our study, many studies of the Z boson LFV decays can be performed in the other BSM and supersymmetric models based on our method for the branching ratios prediction of the LFV observables for the different decay modes.

Acknowledgments

The authors would like to thank the administration of scientific research at Erzincan Binali Yildirim University/Türkiye, Al-Furat and Idlib University/Syria for supporting and funding this work.

A Appendix: Vertexes

A.1 Two Fermions - Z Boson Interactions:

$$\Gamma_{i,j}^{\tilde{\chi}^0 \tilde{\chi}^0 Z, L} = -\frac{i}{2} \left(g_1 \sin \Theta_W + g_2 \cos \Theta_W \right) \left(N_{j3}^* N_{i3} - N_{j4}^* N_{i4} \right) \left(\gamma_\mu \cdot \frac{1 - \gamma_5}{2} \right) \quad (\text{A.1})$$

$$\Gamma_{i,j}^{\tilde{\chi}^0 \tilde{\chi}^0 Z, R} = +\frac{i}{2} \left(g_1 \sin \Theta_W + g_2 \cos \Theta_W \right) \left(N_{i3}^* N_{j3} - N_{i4}^* N_{j4} \right) \left(\gamma_\mu \cdot \frac{1 + \gamma_5}{2} \right) \quad (\text{A.2})$$

$$\Gamma_{i,j}^{\tilde{\chi}^+ \tilde{\chi}^- Z, L} = \frac{i}{2} \left(2g_2 U_{j1}^* \cos \Theta_W U_{i1} + U_{j2}^* \left(-g_1 \sin \Theta_W + g_2 \cos \Theta_W \right) U_{i2} \right) \left(\gamma_\mu \cdot \frac{1 - \gamma_5}{2} \right) \quad (\text{A.3})$$

$$\Gamma_{i,j}^{\tilde{\chi}^+ \tilde{\chi}^- Z, R} = \frac{i}{2} \left(2g_2 V_{i1}^* \cos \Theta_W V_{j1} + V_{i2}^* \left(-g_1 \sin \Theta_W + g_2 \cos \Theta_W \right) V_{j2} \right) \left(\gamma_\mu \cdot \frac{1 + \gamma_5}{2} \right) \quad (\text{A.4})$$

$$\Gamma_{i,j}^{\bar{l} l Z, L} = \frac{i}{2} \delta_{ij} \left(-g_1 \sin \Theta_W + g_2 \cos \Theta_W \right) \left(\gamma_\mu \cdot \frac{1 - \gamma_5}{2} \right) \quad (\text{A.5})$$

$$\Gamma_{i,j}^{\bar{l} l Z, R} = -i g_1 \delta_{ij} \sin \Theta_W \left(\gamma_\mu \cdot \frac{1 + \gamma_5}{2} \right) \quad (\text{A.6})$$

A.2 Two Scalars - Z Boson Interactions:

$$\Gamma_{i,j}^{\nu^I \nu^R Z} = \frac{1}{2} \left(g_1 \sin \Theta_W + g_2 \cos \Theta_W \right) \sum_{a=1}^3 Z_{ia}^{I,*} Z_{ja}^{R,*} \left(-p_\mu^{\nu_j^R} + p_\mu^{\nu_i^I} \right) \quad (\text{A.7})$$

$$\begin{aligned} \Gamma_{i,j}^{\tilde{l} l^* Z} = & \frac{i}{2} \left(-2g_1 \sin \Theta_W \sum_{a=1}^3 Z_{i3+a}^{E,*} Z_{j3+a}^E + \right. \\ & \left. \left(-g_1 \sin \Theta_W + g_2 \cos \Theta_W \right) \sum_{a=1}^3 Z_{ia}^{E,*} Z_{ja}^E \right) \left(-p_\mu^{\tilde{l}_j^*} + p_\mu^{\tilde{l}_i} \right) \end{aligned} \quad (\text{A.8})$$

A.3 Two Fermions - One Scalar Interactions:

$$\begin{aligned} \Gamma_{i,j,k}^{\tilde{\chi}^0 \tilde{l}^*, L} = & i \left(\frac{1}{\sqrt{2}} g_1 N_{i1}^* \sum_{a=1}^3 U_{L,ja}^{l,*} Z_{ka}^E + \frac{1}{\sqrt{2}} g_2 N_{i2}^* \sum_{a=1}^3 U_{L,ja}^{l,*} Z_{ka}^E \right. \\ & \left. - N_{i3}^* \sum_{b=1}^3 U_{L,jb}^{l,*} \sum_{a=1}^3 Y_{l,ab} Z_{k3+a}^E \right) \left(\frac{1 - \gamma_5}{2} \right) \end{aligned} \quad (\text{A.9})$$

$$\Gamma_{i,j,k}^{\tilde{\chi}^0 \tilde{l}^*, R} = + i \left(-\sqrt{2} g_1 \sum_{a=1}^3 Z_{k3+a}^E U_{R,ja}^l N_{i1} - \sum_{b=1}^3 \sum_{a=1}^3 Y_{l,ab}^* U_{R,ja}^l Z_{kb}^E N_{i3} \right) \left(\frac{1 + \gamma_5}{2} \right) \quad (\text{A.10})$$

$$\Gamma_{j,i,k}^{\bar{l} \tilde{\chi}^0 \tilde{e}, L} = i \left(-N_{j3}^* \sum_{b=1}^3 Z_{kb}^{E,*} \sum_{a=1}^3 U_{R,ia}^{l,*} Y_{l,ab} - \sqrt{2} g_1 N_{j1}^* \sum_{a=1}^3 Z_{k3+a}^{E,*} U_{R,ia}^{l,*} \right) \left(\frac{1 - \gamma_5}{2} \right) \quad (\text{A.11})$$

$$\Gamma_{j,i,k}^{\bar{l} \tilde{\chi}^0 \tilde{e}, R} = + i \left(\frac{1}{\sqrt{2}} \sum_{a=1}^3 Z_{ka}^{E,*} U_{L,ia}^l \left(g_1 N_{j1} + g_2 N_{j2} \right) - \sum_{b=1}^3 \sum_{a=1}^3 Y_{l,ab}^* Z_{k3+a}^{E,*} U_{L,ib}^l N_{j3} \right) \left(\frac{1 + \gamma_5}{2} \right) \quad (\text{A.12})$$

$$\Gamma_{i,j,k}^{\bar{l}\tilde{\chi}^-\nu^I,L} = -\frac{1}{\sqrt{2}}U_{j2}^*\sum_{b=1}^3Z_{kb}^{I,*}\sum_{a=1}^3U_{R,ia}^{l,*}Y_{l,ab}\left(\frac{1-\gamma_5}{2}\right) \quad (\text{A.13})$$

$$\begin{aligned} \Gamma_{i,j,k}^{\bar{l}\tilde{\chi}^-\nu^I,R} = & +\frac{1}{4}\left(2\sqrt{2}g_2\sum_{a=1}^3Z_{ka}^{I,*}U_{L,ia}^lV_{j1}\right. \\ & \left.+v_u\left(\sum_{b=1}^3Z_{kb}^{I,*}\sum_{a=1}^3\kappa_{\nu,ab}^*U_{L,ia}^l+\sum_{b=1}^3\sum_{a=1}^3\kappa_{\nu,ab}^*Z_{ka}^{I,*}U_{L,ib}^l\right)V_{j2}\right)\left(\frac{1+\gamma_5}{2}\right) \quad (\text{A.14}) \end{aligned}$$

$$\Gamma_{i,j,k}^{\bar{e}\tilde{\chi}^-\nu^R,L} = i\frac{1}{\sqrt{2}}U_{j2}^*\sum_{b=1}^3Z_{kb}^{R,*}\sum_{a=1}^3U_{R,ia}^{l,*}Y_{l,ab}\left(\frac{1-\gamma_5}{2}\right) \quad (\text{A.15})$$

$$\begin{aligned} \Gamma_{i,j,k}^{\bar{l}\tilde{\chi}^-\nu^R,R} = & +\frac{i}{4}\left(-2\sqrt{2}g_2\sum_{a=1}^3Z_{ka}^{R,*}U_{L,ia}^lV_{j1}\right. \\ & \left.+v_u\left(\sum_{b=1}^3Z_{kb}^{R,*}\sum_{a=1}^3\kappa_{\nu,ab}^*U_{L,ia}^l+\sum_{b=1}^3\sum_{a=1}^3\kappa_{\nu,ab}^*Z_{ka}^{R,*}U_{L,ib}^l\right)V_{j2}\right)\left(\frac{1+\gamma_5}{2}\right) \quad (\text{A.16}) \end{aligned}$$

$$\begin{aligned} \Gamma_{i,j,k}^{\tilde{\chi}^+\nu^I,L} = & \frac{1}{4}\left(-2\sqrt{2}g_2V_{i1}^*\sum_{a=1}^3U_{L,ja}^{l,*}Z_{ka}^{I,*}\right. \\ & \left.-v_uV_{i2}^*\left(\sum_{b=1}^3Z_{kb}^{I,*}\sum_{a=1}^3U_{L,ja}^{l,*}\kappa_{\nu,ab}+\sum_{b=1}^3U_{L,jb}^{l,*}\sum_{a=1}^3Z_{ka}^{I,*}\kappa_{\nu,ab}\right)\right)\left(\frac{1-\gamma_5}{2}\right) \quad (\text{A.17}) \end{aligned}$$

$$\Gamma_{i,j,k}^{\tilde{\chi}^+\nu^I,R} = +\frac{1}{\sqrt{2}}\sum_{b=1}^3Z_{kb}^{I,*}\sum_{a=1}^3Y_{l,ab}^*U_{R,ja}^lU_{i2}\left(\frac{1+\gamma_5}{2}\right) \quad (\text{A.18})$$

$$\begin{aligned} \Gamma_{i,j,k}^{\tilde{\chi}^+e\nu^R,L} = & \frac{i}{4}\left(-2\sqrt{2}g_2V_{i1}^*\sum_{a=1}^3U_{L,ja}^{l,*}Z_{ka}^{R,*}+v_uV_{i2}^*\left(\sum_{b=1}^3Z_{kb}^{R,*}\sum_{a=1}^3U_{L,ja}^{l,*}\kappa_{\nu,ab}\right.\right. \\ & \left.\left.+\sum_{b=1}^3U_{L,jb}^{l,*}\sum_{a=1}^3Z_{ka}^{R,*}\kappa_{\nu,ab}\right)\right)\left(\frac{1-\gamma_5}{2}\right) \quad (\text{A.19}) \end{aligned}$$

$$\Gamma_{i,j,k}^{\tilde{\chi}^+e\nu^R,R} = +i\frac{1}{\sqrt{2}}\sum_{b=1}^3Z_{kb}^{R,*}\sum_{a=1}^3Y_{l,ab}^*U_{R,ja}^lU_{i2}\left(\frac{1+\gamma_5}{2}\right) \quad (\text{A.20})$$

A.4 Two Scalars - γ Interactions:

$$\frac{i}{2}\left(2g_1\cos\Theta_W\sum_{a=1}^3Z_{i3+a}^{E,*}Z_{j3+a}^E+\left(g_1\cos\Theta_W+g_2\sin\Theta_W\right)\sum_{a=1}^3Z_{ia}^{E,*}Z_{ja}^E\right)\left(-p_\mu^{\tilde{e}_j^*}+p_\mu^{\tilde{e}_i}\right) \quad (\text{A.21})$$

A.5 Two Fermions - γ Interactions:

$$\frac{i}{2} \left(2g_2 U_{j1}^* \sin \Theta_W U_{i1} + U_{j2}^* \left(g_1 \cos \Theta_W + g_2 \sin \Theta_W \right) U_{i2} \right) \left(\gamma_\mu \cdot \frac{1 - \gamma_5}{2} \right) \quad (\text{A.22})$$

$$+ \frac{i}{2} \left(2g_2 V_{i1}^* \sin \Theta_W V_{j1} + V_{i2}^* \left(g_1 \cos \Theta_W + g_2 \sin \Theta_W \right) V_{j2} \right) \left(\gamma_\mu \cdot \frac{1 + \gamma_5}{2} \right) \quad (\text{A.23})$$

References

- [1] R. Primulandoando, J. Julio and P. Uttayarat, *Scalar phenomenology in type-ii seesaw model*, *J. High Energ. Phys.* **02** (2022) [[arXiv:1903.02493](#)].
- [2] Z. Li and F. Wang, *Type-ii neutrino seesaw mechanism extension of nmssm from susy breaking mechanisms*, *Eur. Phys. J. C* **80** (2020) [[arXiv:2001.04155](#)].
- [3] SUPER-KAMIOKANDE collaboration, *Evidence for oscillation of atmospheric neutrinos*, *Phys. Rev. Lett.* **81** (1998) 1562.
- [4] SNO collaboration, *Direct evidence for neutrino flavor transformation from neutral-current interactions in the sudbury neutrino observatory*, *Phys. Rev. Lett.* **89** (2002) 011301 [[arXiv:nucl-ex/0204008](#)].
- [5] KAMLAND collaboration, *First results from kamland: Evidence for reactor anti-neutrino disappearance*, *Phys. Rev. Lett.* **90** (2003) 021802 [[arXiv:hep-ex/0212021](#)].
- [6] KAMLAND collaboration, *Precision measurement of neutrino oscillation parameters with kamland*, *Phys. Rev. Lett.* **100** (2008) 221803 [[arXiv:0801.4589](#)].
- [7] X.-X. Dong, S.-M. Zhao, X.-J. Zhan, Z.-J. Yang, H.-B. Zhang and T.-F. Feng, *$Z \rightarrow l_i^\pm l_j^\pm$ processes in the blmssm*, *Chinese Physics C* **41** (2017) 073103 [[arXiv:1704.02202](#)].
- [8] KATRIN collaboration, *Analysis methods for the first katrin neutrino-mass measurement*, *Phys. Rev. D* **104** (2021) 012005 [[arXiv:2101.05253](#)].
- [9] KATRIN collaboration, *First direct neutrino-mass measurement with sub-eV sensitivity*, *Nature Physics* **18** (2022) 160 [[arXiv:2105.08533](#)].
- [10] M. Hirsch, F.R. Joaquim and A. Vicente, *Constrained susy seesaws with a 125 gev higgs*, *J. High Energ. Phys.* **2012** (2012) [[arXiv:1207.6635](#)].
- [11] J. Esteves, M. Hirsch, W. Porod, J. Romao, J. Valle and A. Villanova del Moral, *Flavour violation at the lhc: type-i versus type-ii seesaw in minimal supergravity*, *J. High Energ. Phys.* **2009** (2009) [[arXiv:0903.1408](#)].
- [12] S. Weinberg, *Baryon- and lepton-nonconserving processes*, *Phys. Rev. Lett.* **43** (1979) 1566.
- [13] S. Weinberg, *Varieties of baryon and lepton nonconservation*, *Phys. Rev. D* **22** (1980) 1694.
- [14] P. Minkowski, $\mu \rightarrow e \gamma$ at a rate of one out of 109 muon decays?, *Physics Letters B* **67** (1977) 421.
- [15] T. Yanagida, *Proc. workshop on unified theory and the baryon number in the universe*, KEK Report No. 79-18 **95** (1979) .
- [16] M. Gell-Mann, *Talk given at the 1977 washington meeting of the american physical society. see also, m. gell-mann, p. ramond and r. slansky, "supergravity", in Proc. of the Supergravity Workshop at Stony Brook, eds P. van Nieuwenhuizen and DZ Freedman (North Holland Publ. Co., Amsterdam, 1979), p. 315.*

- [17] R.N. Mohapatra and G. Senjanović, *Neutrino mass and spontaneous parity nonconservation*, [*Phys. Rev. Lett.* **44** \(1980\) 912](#).
- [18] J. Schechter and J.W.F. Valle, *Neutrino masses in $su(2) \otimes u(1)$ theories*, [*Phys. Rev. D* **22** \(1980\) 2227](#).
- [19] J. Schechter and J.W.F. Valle, *Neutrino decay and spontaneous violation of lepton number*, [*Phys. Rev. D* **25** \(1982\) 774](#).
- [20] W. Konetschny and W. Kummer, *Nonconservation of total lepton number with scalar bosons*, [*Physics Letters B* **70** \(1977\) 433](#).
- [21] R.E. Marshak and R.N. Mohapatra, *Selection rules for baryon number nonconservation in gauge models*, in *Recent Developments in High-Energy Physics*, A. Perlmutter and L.F. Scott, eds., (Boston, MA), pp. 277–287, Springer US (1980), [DOI](#).
- [22] T.P. Cheng and L.-F. Li, *Neutrino masses, mixings, and oscillations in $su(2) \times u(1)$ models of electroweak interactions*, [*Phys. Rev. D* **22** \(1980\) 2860](#).
- [23] G. Lazarides, Q. Shafi and C. Wetterich, *Proton lifetime and fermion masses in an $so(10)$ model*, [*Nuclear Physics B* **181** \(1981\) 287](#).
- [24] R.N. Mohapatra and G. Senjanović, *Neutrino masses and mixings in gauge models with spontaneous parity violation*, [*Phys. Rev. D* **23** \(1981\) 165](#).
- [25] L. Basso, A. Belyaev, D. Chowdhury, M. Hirsch, S. Khalil, S. Moretti et al., *Proposal for generalised supersymmetry les houches accord for see-saw models and pdg numbering scheme*, [*Computer Physics Communications* **184** \(2013\) 698](#) [[arXiv:1206.4563](#)].
- [26] R. Foot, H. Lew, X.G. He and G.C. Joshi, *See-saw neutrino masses induced by a triplet of leptons*, [*Zeitschrift für Physik C Particles and Fields* **44** \(1989\) 441](#).
- [27] E. Ma, *Pathways to naturally small neutrino masses*, [*Phys. Rev. Lett.* **81** \(1998\) 1171](#).
- [28] T. Goto, Y. Okada, T. Shindou, M. Tanaka and R. Watanabe, *Lepton flavor violation in the supersymmetric seesaw model after the lhc 8 tev run*, [*Phys. Rev. D* **91** \(2015\) 033007](#) [[arXiv:1412.2530](#)].
- [29] J. Cao, Z. Xiong and J.M. Yang, *Lepton flavor violating z -decays in supersymmetric see-saw model*, [*The European Physical Journal C* **32** \(2004\) 245](#) [[arXiv:hep-ph/0307126](#)].
- [30] D. Jurčiukonis and L. Lavoura, *Two-body lepton-flavour-violating decays in a 2hdm with soft family-lepton-number breaking*, [*J. High Energ. Phys.* **2022** \(2022\)](#) [[arXiv:2107.14207](#)].
- [31] R.S. Hundi, *Lepton flavor violating z and higgs decays in the scotogenic model*, [*Eur. Phys. J. C* **82**,505 \(2022\)](#) [[arXiv:2201.03779](#)].
- [32] ATLAS collaboration, *Search for lepton-flavor violation in z -boson decays with τ leptons with the atlas detector*, [*Phys. Rev. Lett.* **127** \(2021\) 271801](#) [[arXiv:2105.12491](#)].
- [33] ATLAS collaboration, *Search for the charged-lepton-flavor-violating decay $z \rightarrow e\mu$ in pp collisions at $\sqrt{s} = 13$ TeV with the atlas detector*, [*Phys. Rev. D* **108** \(2023\) 032015](#) [[arXiv:2204.10783](#)].
- [34] L. Calibbi, X. Marcano and J. Roy, *Z lepton flavour violation as a probe for new physics at future e^+e^- colliders*, [*Eur. Phys. J. C* **81** \(2021\) 1054](#) [[arXiv:2107.10273](#)].
- [35] G. Bernardi, E. Brost, D. Denisov, G. Landsberg, M. Aleksa, D. d’Enterria et al., *The future circular collider: a summary for the us 2021 snowmass process*, [[arXiv:2203.06520](#)].

- [36] J.I. Illana and M. Masip, *Lepton flavor violation in z and lepton decays in supersymmetric models*, *Phys. Rev. D* **67** (2003) 035004 [[arXiv:hep-ph/0207328](#)].
- [37] M. Hirsch, W. Porod, C. Weiss and F. Staub, *Supersymmetric type-iii seesaw: lepton flavour violation and lhc phenomenology*, *Phys. Rev. D* **87** (2013) 013010 [[arXiv:1211.0289](#)].
- [38] M. Hirsch, S. Kaneko and W. Porod, *Supersymmetric seesaw type ii: Cern lhc and lepton flavour violating phenomenology*, *Phys. Rev. D* **78** (2008) 093004 [[arXiv:0806.3361](#)].
- [39] F. Borzumati and T. Yamashita, *Minimal supersymmetric $su(5)$ model with nonrenormalizable operators: Seesaw mechanism and violation of flavour and cp* , *Progress of Theoretical Physics* **124** (2010) 761 [[arXiv:0903.2793](#)].
- [40] A. Abada, A.J.R. Figueiredo, J.C. Romão and A.M. Teixeira, *Probing the supersymmetric type iii seesaw: Lfv at low-energies and at the lhc*, *J. High Energy. Phys.* **2011** (2011) [[arXiv:1104.3962](#)].
- [41] J.N. Esteves, J.C. Romao, M. Hirsch, F. Staub and W. Porod, *Supersymmetric type-iii seesaw: lepton flavour violating decays and dark matter*, *Phys. Rev. D* **83** (2011) 013003 [[arXiv:1010.6000](#)].
- [42] A. Vicente, *Lepton flavor violation beyond the mssm*, *Advances in High Energy Physics* **2015** (2015) 22 [[arXiv:1503.08622](#)].
- [43] M.D. Goodsell, K. Nickel and F. Staub, *Two-loop higgs mass calculations in supersymmetric models beyond the mssm with sarah and spheno*, *Eur. Phys. J. C* **75** (2015) [[arXiv:1411.0675](#)].
- [44] J. Bernigaud, A.K. Forster, B. Herrmann, S.F. King, W. Porod and S.J. Rowley, *Data-driven analysis of a susy gut of flavour*, *J. High Energy. Phys.* **2022** (2022) [[arXiv:2111.10199](#)].
- [45] W. Porod, F. Staub and A. Vicente, *A flavor kit for bsm models*, *Eur. Phys. J. C* **74** (2014) [[arXiv:1405.1434](#)].
- [46] G. D'Ambrosio, T. Hambye, A. Hektor, M. Raidal and A. Rossi, *Leptogenesis in the minimal supersymmetric triplet seesaw model*, *Physics Letters B* **604** (2004) 199 [[arXiv:hep-ph/0407312](#)].
- [47] F. Joaquim and A. Rossi, *Phenomenology of the triplet seesaw mechanism with gauge and yukawa mediation of susy breaking*, *Nuclear Physics B* **765** (2007) 71 [[arXiv:hep-ph/0607298](#)].
- [48] A. Rossi, *Supersymmetric seesaw without singlet neutrinos: Neutrino masses and lepton-flavour violation*, *Phys. Rev. D* **66** (2002) 075003 [[arXiv:hep-ph/0207006](#)].
- [49] C. CSÁKI, *The minimal supersymmetric standard model (mssm)*, *Modern Physics Letters A* **11** (1996) 599 [[arXiv:hep-ph/9606414](#)].
- [50] J. Yang, *Lepton flavor violating z -boson decays at gigaz as a probe of supersymmetry*, *Science China Physics, Mechanics and Astronomy* **53** (2010) 1949 [[arXiv:1006.2594](#)].
- [51] V. De Romeri, M. Herrero, X. Marcano and F. Scarcella, *Lepton flavor violating z decays: A promising window to low scale seesaw neutrinos*, *Phys. Rev. D* **95** (2017) 075028 [[arXiv:1607.05257](#)].
- [52] X. Marcano, *Lepton Flavor Violation from Low Scale Seesaw Neutrinos with Masses Reachable at the LHC*, Springer Cham (2018), [10.1007/978-3-319-94604-7](#).

- [53] K.-S. Sun, J.-B. Chen, X.-Y. Yang and S.-K. Cui, *The lfv decays of z boson in minimal r-symmetric supersymmetric standard model*, *Chinese Physics C* **43** (2019) 043101 [[arXiv:1901.03800](#)].
- [54] X.-J. Bi, Y.-B. Dai and X.-Y. Qi, *Lepton flavor violation in supersymmetric so(10) grand unified models*, *Phys. Rev. D* **63** (2001) 096008 [[arXiv:hep-ph/0010270](#)].
- [55] S. Navas, C. Amsler, T. Gutsche, C. Hanhart, J.J. Hernández-Rey, C. Lourenço et al., *Review of particle physics*, *Phys. Rev. D* **110** (2024) 030001.
- [56] G. Passarino and M. Veltman, *One-loop corrections for e^+e^- annihilation into $\mu^+\mu^-$ in the weinberg model*, *Nuclear Physics B* **160** (1979) 151.
- [57] T. Hahn, *Automatic loop calculations with feynarts, formcalc, and looptools*, *Nuclear Physics B - Proceedings Supplements* **89** (2000) 231 [[arXiv:hep-ph/0005029](#)].
- [58] H.H. Patel, *Package-x: A mathematica package for the analytic calculation of one-loop integrals*, *Computer Physics Communications* **197** (2015) 276 [[arXiv:1503.01469](#)].
- [59] F. Staub, *From superpotential to model files for feynarts and calchep/comphep*, *Computer Physics Commun.* **181** (2010) 1077 [[arXiv:0909.2863](#)].
- [60] F. Staub, *Sarah 4: A tool for (not only susy) model builders*, *Computer Physics Commun.* **185** (2014) 1773 [[arXiv:1309.7223](#)].
- [61] BELLE collaboration, *Search for lepton-flavor-violating tau-lepton decays to $\ell\gamma$ at belle*, *J. High Energ. Phys.* **2021** (2021) [[arXiv:2103.12994](#)].
- [62] MEG collaboration, *Search for the lepton flavour violating decay $\mu^+ \rightarrow e^+ \gamma$ with the full dataset of the meg experiment*, *Eur. Phys. J. C* **76** (2016) [[arXiv:1605.05081](#)].
- [63] J. Hisano, T. Moroi, K. Tobe and M. Yamaguchi, *Lepton-flavor violation via right-handed neutrino yukawa couplings in supersymmetric standard model*, *Phys. Rev. D* **53** (1996) 2442 [[arXiv:hep-ph/9510309](#)].